

# Global Biogeochemical Cycles

## RESEARCH ARTICLE

10.1029/2020GB006707

### Key Points:

- We identify an imbalance in Earth's early carbon budget, with inputs exceeding outputs
- This discrepancy can be resolved by invoking higher organic burial efficiency
- Higher burial efficiency can be reconciled with an anoxic Archean atmosphere if outgassing of reductants from the mantle was greater than today

### Supporting Information:

- Supporting Information S1

### Correspondence to:

M. A. Kipp,  
[mkipp@caltech.edu](mailto:mkipp@caltech.edu)

### Citation:

Kipp, M., Krissansen-Totton, J., & Catling, D. C. (2021). High organic burial efficiency is required to explain mass balance in earth's early carbon cycle. *Global Biogeochemical Cycles*, 35, e2020GB006707. <https://doi.org/10.1029/2020GB006707>

Received 16 JUN 2020

Accepted 17 DEC 2020

## High Organic Burial Efficiency Is Required to Explain Mass Balance in Earth's Early Carbon Cycle

Michael A. Kipp<sup>1,2,3</sup> , Joshua Krissansen-Totton<sup>1,2,4,5</sup> , and David C. Catling<sup>1,2</sup> 

<sup>1</sup>Department of Earth & Space Sciences and Astrobiology Program, University of Washington, Seattle, WA, USA, <sup>2</sup>Virtual Planetary Laboratory, NASA Nexus for Exoplanet System Science, Seattle, WA, USA, <sup>3</sup>Division of Geological & Planetary Sciences, California Institute of Technology, Pasadena, CA, USA, <sup>4</sup>Department of Astronomy and Astrophysics, University of California, Santa Cruz, CA, USA, <sup>5</sup>NASA Sagan Fellow

**Abstract** Earth's carbon cycle maintains a stable climate and biosphere on geological timescales. Feedbacks regulate the size of the surface carbon reservoir, and on million-year timescales the carbon cycle must be in steady state. A major question about the early Earth is whether carbon was cycled through the surface reservoir more quickly or slowly than it is today. The answer to this question holds important implications for Earth's climate state, the size of the biosphere through time, and the expression of atmospheric biosignatures on Earth-like planets. Here, we examine total carbon inputs and outputs from the Earth's surface over time. We find stark disagreement between the canonical histories of carbon outgassing and carbon burial, with the former implying high rates of throughput on the early Earth and the latter suggesting sluggish carbon cycling. We consider solutions to this apparent paradox and conclude that the most likely resolution is that high organic burial efficiency in the Precambrian enabled substantial carbon burial despite limited biological productivity. We then consider this model in terms of Archean redox balance and find that in order to maintain atmospheric anoxia prior to the Great Oxidation Event, high burial efficiency likely needed to be accompanied by greater outgassing of reductants. Similar mechanisms likely govern carbon burial and redox balance on terrestrial exoplanets, suggesting that outgassing rates and the redox state of volcanic gases likely play a critical role in setting the tempo of planetary oxygenation.

### 1. Introduction

Earth holds vast reservoirs of carbon in the crust and mantle, dwarfing the amount that is held in the surface reservoir (i.e., the atmosphere, ocean and biosphere) (Catling & Kasting, 2017). The input of carbon to the surface reservoir is carefully balanced by outputs because marginal excess of outputs would lead to depletion of atmospheric CO<sub>2</sub>, and marginal excess of inputs would lead to implausibly high levels of CO<sub>2</sub>, both on ~1 Myr timescales (Berner & Caldeira, 1997). Thus, negative feedbacks stabilize Earth's carbon cycle on >1 Myr timescales, keeping inputs and outputs balanced, thereby avoiding dramatic warming or cooling events.

While it is clear that mass balance must hold between carbon inputs and outputs on geological timescales, can we determine the throughput of carbon in deep time—that is, the rate at which carbon was added to and removed from the surface reservoir? Doing so is critical for understanding Earth's evolution as a habitable planet, particularly since biogeochemical modulation of greenhouse gas (i.e., CO<sub>2</sub> and CH<sub>4</sub>) concentrations has played an important role in regulating Earth's climate since at least the Archean (Kharecha et al., 2005; Krissansen-Totton et al., 2018a), and perhaps Hadean (Kadoya et al., 2020a). It also would help us to more accurately model the expression of atmospheric biosignatures on the early Earth (Krissansen-Totton et al., 2018b; Stüeken et al., 2016), which is relevant to the detectability of life on Earth-like exoplanets (Reinhard et al., 2017a).

In its simplest form, the carbon budget of the Earth's surface reservoir at steady state can be expressed

$$C_{\text{total\_input}} = C_{\text{total\_burial}} \quad (1)$$

on >1 Myr timescales (Berner & Caldeira, 1997). Here, we assess Earth's early carbon budget and find a stark disagreement between canonical models of evolving carbon inputs and outputs. Specifically, most

studies of Earth's geothermal evolution invoke greater carbon inputs early in Earth's history due to elevated outgassing rates, yet most studies of carbon burial imply lower rates due to diminished biological productivity and near-modern fractional organic carbon burial. We consider various solutions to this paradox, finding that high burial efficiency of organic carbon in Precambrian marine sediments provides the most compelling explanation for mass balance in Earth's early carbon cycle. We then assess the effect of high burial efficiency on Earth's redox budget prior to the Great Oxidation Event (GOE), considering also the implications for atmospheric oxygenation on Earth-like exoplanets.

## 2. The Early Earth Productivity Paradox

We approach the problem by breaking each flux into its components, drawing from the frameworks outlined by Holland (1984, p. 180) and Berner (2004, p. 10). We then reconstruct the temporal evolution of each individual component and sum those components to estimate  $C_{\text{total\_input}}$  and  $C_{\text{total\_burial}}$  across Earth's history. To begin, we consider only *relative* changes in each component flux. After determining the relative magnitude of each flux over Earth's history ( $R_{\text{flux}}$ ), we then use estimates of absolute fluxes on the modern Earth ( $C_{\text{flux}}^{\text{modern}}$ ) to assess the implications for carbon cycle mass balance through time.

Beginning with the input side of the equation, the two routes of carbon input to the surface reservoir are volcanism (i.e., outgassing) and weathering, such that

$$C_{\text{total\_input}} = C_{\text{total\_outgassing}} + C_{\text{total\_weathering}} \quad (2)$$

Each of these sources can, in turn, be split into two components. Volcanic carbon inputs derive from mantle outgassing (i.e., emanation of carbon from the mantle at mid-ocean ridges or intraplate settings) and metamorphic outgassing (i.e., volatilization and release of sedimentary carbon entering subduction zones or collisional regimes), such that

$$C_{\text{total\_outgassing}} = C_{\text{mantle\_outgassing}} + C_{\text{metamorphic\_outgassing}} \quad (3)$$

Crustal weathering accesses two pools of carbon: carbonate minerals and sedimentary organic matter, such that

$$C_{\text{total\_weathering}} = C_{\text{carb\_weathering}} + C_{\text{org\_weathering}} \quad (4)$$

Let us first consider  $C_{\text{mantle\_outgassing}}$ . Since the mantle is a nearly infinite reservoir of carbon relative to the outgassing flux (there are  $\sim 10^{22}$  moles of carbon in the mantle versus  $\sim 10^{12}$  moles of carbon outgassed from the mantle per year; Dasgupta & Hirschmann, 2010), the rate of carbon outgassing from the mantle is primarily related to heat flow (i.e., the rate of mantle volcanism, which occurs in both mid-ocean ridge and intraplate settings; Lee et al., 2016). Several models describe Earth's geothermal evolution. While there is considerable spread in their predictions, all models invoke relative heat flow ( $Q$ ) on the early Earth that is comparable to or greater than modern (Figure 1a). Following Krissansen-Totton et al. (2018a), we use these heat flow estimates to calculate relative changes in mantle outgassing across Earth's history as

$$R_{\text{mantle\_outgassing}} = \frac{C_{\text{mantle\_outgassing}}}{C_{\text{mantle\_outgassing}}^{\text{modern}}} = Q^m \quad (5)$$

where  $m$  between 0 and 2 represents the full range of possible geodynamic scenarios. In doing so, we find that mantle outgassing rates may have been much higher in Earth's early history than at present (blue shaded region, Figure 1b), perhaps by an order of magnitude or more in the early Archean.

Estimating the other route of carbon outgassing,  $C_{\text{metamorphic\_outgassing}}$ , is more complicated. In addition to depending on relative heat flow, metamorphic devolatilization of sedimentary carbon in arc regions depends on the amount of sedimentary carbon entering subduction zones worldwide (Lee et al., 2016). This means that the size of the crustal carbon reservoir, paleogeographic, and tectonic state of the Earth system, and

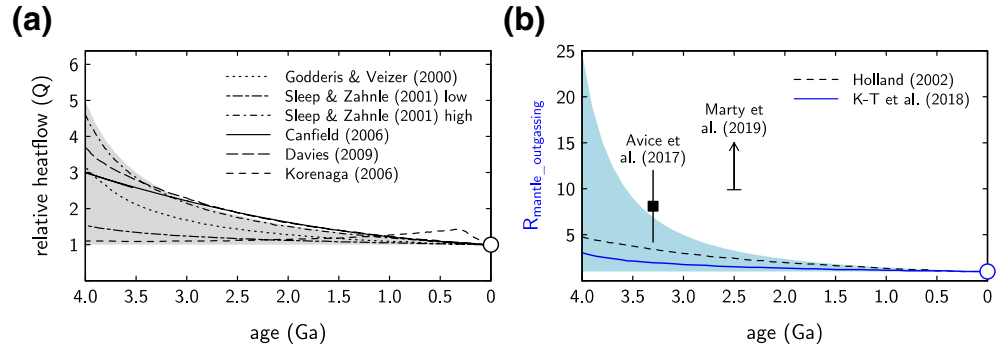


**Figure 1.** Relative evolution of heat flow and mantle outgassing of carbon through Earth's history. Individual lines in panel (a) denote different models of heat flow evolution. Gray shaded region in panel (a) denotes range utilized for calculation of  $R_{\text{mantle\_outgassing}}$  in panel (b). Solid blue line in panel (b) denotes nominal model output of Krissansen-Totton et al. (2018a); dashed black line denotes model of Holland (2002). Black symbols in panel (b) represent empirical constraints on mantle outgassing based on Xe isotope systematics (discussed in Section 3.1). White circles in these and subsequent plots represent modern flux values.

relative heat flow can all play a role in setting the rate of  $C_{\text{metamorphic\_outgassing}}$ . The situation is further complicated by the fact that some authors have suggested preferential subduction of organic carbon relative to carbonate under the steeper geothermal gradient inferred for the early Earth (Duncan & Dasgupta, 2017).

Here, we adopt a simple parameterization to calculate plausible end-member trajectories for metamorphic outgassing through Earth's history. To do so, we scale the modern flux by relative heat flow and the relative size of the continental carbon (carbonate + organic carbon) reservoir,  $f_{\text{cont}}$ , where a value of 1 represents the modern reservoir size

$$R_{\text{metamorphic\_outgassing}} = \frac{C_{\text{metamorphic\_outgassing}}}{C_{\text{metamorphic\_outgassing}}^{\text{modern}}} = Q^m f_{\text{cont}} \quad (6)$$

In one end-member scenario, we assume that the continents quickly reached steady-state with respect to their carbon reservoir (i.e.,  $f_{\text{cont}} = 1$  through Earth's history). In the other case, we assume that the continental carbon reservoir has steadily grown through time (Lee et al., 2016) (Figure 2a). We then multiply each of these trajectories by the full range of heat flow histories (Figure 1a) to obtain an uncertainty range for  $R_{\text{metamorphic\_outgassing}}$  (blue shaded region, Figure 2b). This calculation shows that metamorphic outgassing rates were likely within an order of magnitude of the modern flux for most of Earth's history.

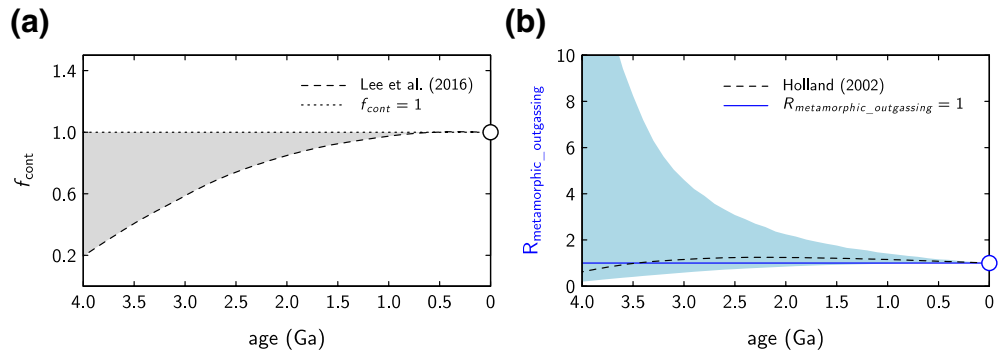


**Figure 2.** Evolution of continental carbon reservoir and  $R_{\text{metamorphic\_outgassing}}$  through Earth's history. Dashed line in panel (a) denotes continental carbon reservoir evolution of Lee et al. (2016); dotted line represents end-member scenario of constant carbon reservoir size. Gray shaded region in panel (a) denotes range of values used to obtain range of  $R_{\text{metamorphic\_outgassing}}$  values shown in panel (b) as the blue shaded region. Solid blue line in panel (b) represents conservative estimate of constant metamorphic outgassing rates; dashed line represents model output of Holland (2002).

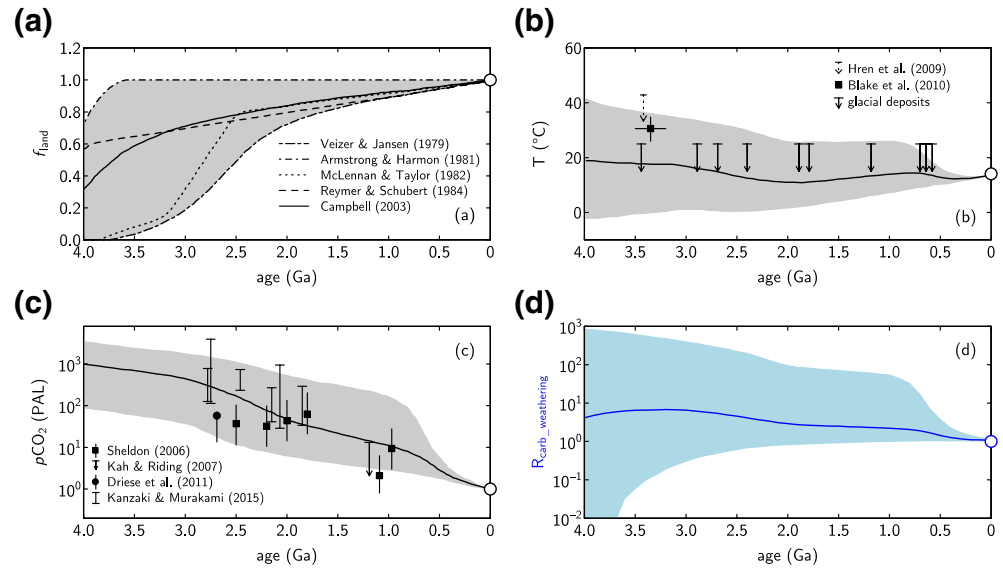


**Figure 3.** (a) Temporal evolution of emerged landmass area, (b) global mean surface temperature, (c) atmospheric CO<sub>2</sub> levels, and (d) relative carbonate weathering. Individual lines in panel (a) represent different models of continental emergence; gray shaded region denotes range used to calculate range of carbonate weathering values in panel (d). Symbols in panels (b) and (c) denote empirical constraints on surface temperature and pCO<sub>2</sub>, respectively. Gray shaded regions in panels (b) and (c) denote 95% confidence interval in model outputs of Krissansen-Totton et al. (2018a); solid black lines denote median output. Since these ranges broadly encompass the empirical constraints in the literature, we use them to calculate the range of plausible carbonate weathering fluxes in panel (d). The solid line in panel (d) is calculated using the solid line trajectories in panels (a–c).

In this simple formulation, we neglect the possibility that previous intervals of Earth's history featured larger-than-modern fluxes of sedimentary carbon into subduction zones (e.g., the Cretaceous, Krissansen-Totton et al., 2017; Lee et al., 2016; Ramos et al., 2020), meaning that we could be underestimating metamorphic outgassing in such intervals. However, here we are primarily concerned with carbon cycling in the Precambrian—when the sparse geologic record precludes high-resolution studies of metamorphic decarbonation signatures in subduction zone relics (e.g., Ramos et al., 2020). So, we find our simple approximation to be reasonably representative of the uncertainty surrounding estimates of metamorphic outgassing on this time scale and also conservative given our attempt to demonstrate that carbon inputs exceed inferred burial rates in the Precambrian.

We now turn to weathering, considering first  $C_{\text{carb\_weathering}}$ . Like silicate weathering, carbonate weathering depends on both pCO<sub>2</sub> and temperature (Berner, 2004), though the precise quantitative relationship between each parameter remains uncertain (e.g., Gaillardet et al., 2019; Romero-Mujalli et al., 2019). In addition to climatic parameters, on geologic timescales weathering rates also depend on the area of land that is exposed to subaerial weathering (cf., Krissansen-Totton et al., 2018a) and the relative proportion of that land that is covered by carbonates (Bluth & Kump, 1991). To calculate the influence of each of these parameters on carbonate weathering rates through time, we follow Krissansen-Totton et al. (2017) by modifying the silicate weathering expression of Walker et al. (1981; their Equation 1) to describe relative carbonate weathering as

$$R_{\text{carb\_weathering}} = \frac{C_{\text{carb\_weathering}}}{C_{\text{carb\_weathering}}^{\text{modern}}} = f_{\text{land}} \left( \frac{p_{\text{CO}_2}}{p_{\text{CO}_2}^{\text{modern}}} \right)^{\alpha} \exp \left( \frac{T - T_{\text{modern}}}{T_e} \right) \quad (7)$$

Here,  $f_{\text{land}}$  represents the relative extent of emerged crust (ranging from 0 to 1, with 1 representing modern emergent land area). We do not separately parameterize the proportion of carbonate on land, though we effectively consider lower values for this variable by sampling very low estimates of continental emergence (Figure 3a). The CO<sub>2</sub>-dependence of carbonate weathering is parameterized as relative pCO<sub>2</sub>

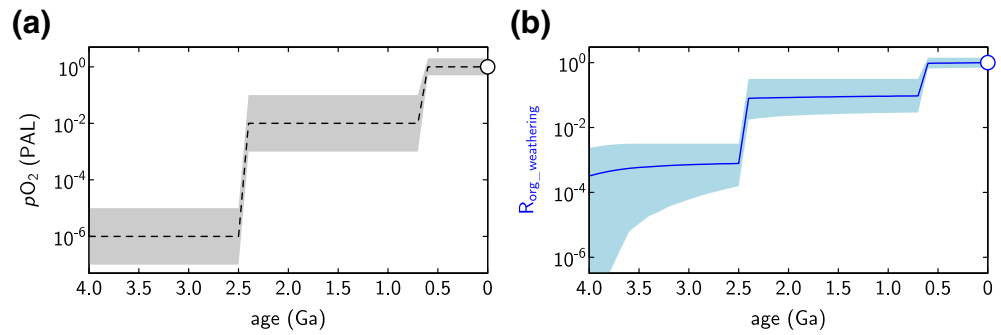


**Figure 4.** (a) Evolution of atmospheric oxygen levels and (b) the organic carbon weathering flux. Atmospheric oxygen trajectory in panel (a) is a simplified version of the oxygen history reviewed in Lyons et al. (2014). The gray shaded region was used to calculate the range of plausible organic weathering fluxes (blue shaded region in panel b), while the dashed black line was used to calculate the solid blue line.

scaled by a factor,  $\alpha$ . While estimates of  $\alpha$  remain uncertain, we sample a broad range of values (0.2–0.5; Krissansen-Totton et al., 2017) in order to account for weak or strong  $\text{CO}_2$ -dependence of carbonate weathering. The final term captures the temperature-dependence of carbonate weathering, where  $T$  is the global mean surface temperature,  $T_{\text{modern}}$  is the modern surface temperature (285 K), and  $T_e$  is the e-folding temperature. We sample a broad range of  $T_e$  values (10–40 K; Krissansen-Totton et al., 2017; 2018a) to encompass both a weak and strong temperature-dependence of carbonate weathering (for instance, sampling this range accounts for uncertainty in our understanding of the relationship between temperature and precipitation). We note that this range of  $T_e$  values was derived for silicate weathering; it is possible that carbonate weathering could show an even stronger temperature dependence, that is,  $T_e < 10$  K, but this would only further elevate carbon inputs, exacerbating the budget imbalance we are identifying here.

We consider a wide range of model histories for  $f_{\text{land}}$  (Figure 3a). For  $p\text{CO}_2$  and  $T$ , we adopt the full range of model outputs from Krissansen-Totton et al. (2018a) (gray shaded regions in Figures 3b) and 3c). These ranges encompass empirical estimates for each parameter, suggesting that they indeed capture plausible end-member scenarios. We then use the full range of uncertainty on each parameter (gray shaded regions in Figures 3a–3c) to calculate a plausible history of carbonate weathering (blue shaded region in Figure 3d). We find that uncertainty in carbonate weathering rates spans more than an order of magnitude in Earth’s early history, though most of the available parameter space invokes higher-than-modern carbonate weathering in the Precambrian due to elevated  $p\text{CO}_2$ .

Next we consider  $C_{\text{org\_weathering}}$ . As with carbonate weathering, the rate of organic weathering depends on the extent of emerged land. However, it is the atmospheric oxygen level ( $p\text{O}_2$ ) rather than  $p\text{CO}_2$  that influences organic weathering rates (Bolton et al., 2006). Some authors have used this logic to argue that organic weathering was much less effective in the Precambrian than today, as the kinetics of organic matter oxidation would be more sluggish under lower atmospheric oxygen concentrations (Bekker & Holland, 2012; Daines et al., 2017). We calculate organic weathering rates as

$$R_{\text{org\_weathering}} = \frac{C_{\text{org\_weathering}}}{C_{\text{org\_weathering}}^{\text{modern}}} = f_{\text{land}} \left( \frac{p\text{O}_2}{p\text{O}_2^{\text{modern}}} \right)^z \quad (8)$$

Using the range of  $f_{\text{land}}$  estimates (Figure 3a), a  $z$  value of 0.5 (Chang & Berner, 1999; Daines et al., 2017; Lasaga & Ohmoto, 2002), and a simplified history of atmospheric oxygen (Figure 4a) based on a recent review of redox proxy data (Lyons et al., 2014), we calculate the plausible evolution of organic weathering rates across Earth’s history (blue shaded region in Figure 4b). This calculation reveals that organic weathering would indeed have been a negligible contributor to C cycle mass balance on the early Earth due to atmospheric oxygen levels that were orders of magnitude lower than today.

With all of the carbon input components constrained, we now turn to the carbon burial side of the equation. Carbon is buried in both inorganic (carbonate) and organic forms, such that total burial can be calculated

$$C_{\text{total\_burial}} = C_{\text{carb\_burial}} + C_{\text{org\_burial}} \quad (9)$$

The relative contribution of these two burial pathways is often expressed by the variable,  $f_{\text{org}}$

$$f_{\text{org}} = \frac{C_{\text{org\_burial}}}{C_{\text{total\_burial}}} \quad (10)$$

which describes the fraction of total carbon burial accounted for by organic carbon. An advantage of this approach is that total carbon burial can be determined if only one component (*either* organic or carbonate) is known, in addition to  $f_{\text{org}}$ .

The value of  $f_{\text{org}}$  is thought to be recorded in the carbon isotopic composition of sedimentary carbonates and organic matter that are preserved across Earth's history. In the canonical framework, the rate of organic carbon burial (which is accompanied by a large isotopic fractionation, typically about  $-25\%$ ; Krissansen-Totton et al., 2015; Schidlowski, 2001) controls the isotopic enrichment in inorganic carbon (i.e., marine carbonates), such that  $f_{\text{org}}$  can be calculated

$$f_{\text{org}} = \frac{(\delta^{13}\text{C}_{\text{carb}} - \delta^{13}\text{C}_{\text{input}})}{(\delta^{13}\text{C}_{\text{carb}} - \delta^{13}\text{C}_{\text{org}})} \quad (11)$$

Here,  $\delta^{13}\text{C}_{\text{input}}$  is estimated at  $-5\%$  based on analyses of basalts (Mattey, 1987), xenoliths (Deines, 2002; Mattey, 1987; Pearson et al., 2014) and diamonds (Cartigny, 2005; Shirey et al., 2013) that are all thought to record the composition of the upper mantle.

Compilations of  $\delta^{13}\text{C}$  values in carbonates and sedimentary organic matter across Earth's history have been used to calculate  $f_{\text{org}}$  through time (Des Marais et al., 1992; Krissansen-Totton et al., 2015). If we assume, as many authors have, that the carbon isotopic record allows a robust reconstruction of fractional organic carbon burial in deep time (an assumption that will be critically evaluated in Section 4.1), we will be able to determine  $C_{\text{total\_burial}}$  if we can obtain constraints on  $C_{\text{org\_burial}}$ .

The rate of organic carbon burial depends on two things: the annual production of organic carbon (net primary productivity, NPP) and the efficiency with which that organic carbon is buried (burial efficiency,  $\varepsilon_b$ ), such that the rate relative to modern is

$$R_{\text{org\_burial}} = \frac{C_{\text{org\_burial}}}{C_{\text{org\_burial}}^{\text{modern}}} = \left( \frac{\text{NPP}}{\text{NPP}^{\text{modern}}} \right) \left( \frac{\varepsilon_b}{\varepsilon_b^{\text{modern}}} \right) \quad (12)$$

We use a single term ( $\varepsilon_b$ ) to describe burial efficiency here, though we note that in the oceanographic literature (see, e.g., Hedges & Keil, 1995; Middelburg, 2019) this value is typically broken into two parameters: export efficiency (the fraction of NPP that reaches sediments) and preservation efficiency (the fraction of exported organic carbon that ultimately gets buried with sediments). As we have no means to distinguish between these two parameters in deep time, we follow others (e.g., Laakso & Schrag, 2018) in simplifying our treatment by considering a single term for net burial efficiency ( $\varepsilon_b$ ), which is the product of export efficiency and preservation efficiency.

Assuming for the moment that  $\varepsilon_b$  has been constant (i.e.,  $\varepsilon_b = \varepsilon_b^{\text{modern}}$ ) throughout Earth's history (an assumption that will be critically evaluated in Section 5), organic burial scales directly with changes in NPP. Several lines of evidence have been used to suggest that NPP was lower in Earth's early history (reviewed in Section 4.2). Using these estimates of relative NPP in deep time (Figure 5a), we calculated  $R_{\text{org\_burial}}$  using Equation 12. This reveals that organic burial should have been lower in the Precambrian due to diminished productivity (red shaded region in Figure 5b). We then use this organic burial history and a reconstruction

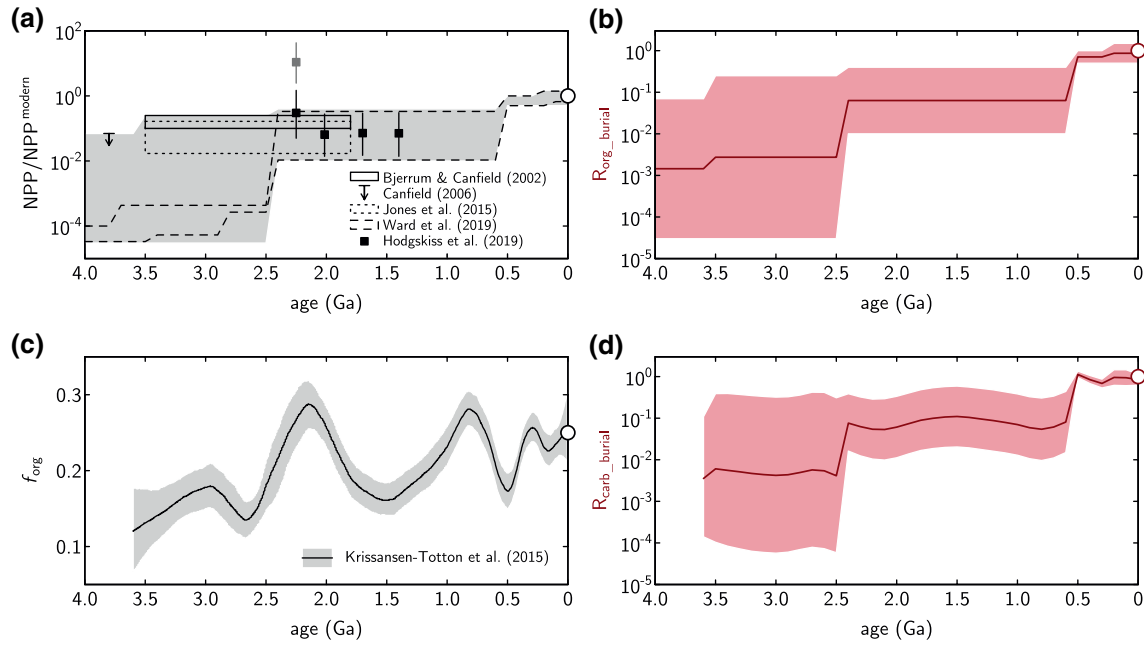


**Figure 5.** (a) Evolution of net primary production, (b) relative organic carbon burial, assuming constant  $\epsilon_b$ , (c) fractional organic burial, and (d) relative carbonate burial. Symbols in panel (a) represent empirical and theoretical constraints on NPP; gray shaded region represents the range of values used to calculate the range of organic burial fluxes shown as the red shaded region in panel (b). Solid black line in panel (c) denotes  $f_{org}$  reconstruction of Krissansen-Totton et al. (2015); gray shaded region denotes 95% confidence interval, which was used to calculate range of carbonate burial fluxes shown as red shaded region in panel (d). Solid red lines in panels (b) and (d) denote the geometric mean of the maximum and minimum values.

of  $f_{org}$  from the carbon isotope record (Figure 5c; Krissansen-Totton et al., 2015) to calculate carbonate burial via Equation 10. The result is the red shaded region in Figure 5d.

Having now tabulated estimates of the relative magnitude of each flux over Earth's history, we can consider whether these reconstructions are consistent with carbon cycle mass balance. This requires that we scale all of the relative flux terms ( $R_{flux}$ ) by their modern absolute flux ( $C_{flux}^{modern}$ ). As with the determination of the relative evolution of each flux through time, considerable uncertainty surrounds the estimation of absolute fluxes on the modern Earth. Several authors have assembled tabulations of modern fluxes, each with slightly different implications for the trajectory of carbon inputs and outputs across Earth's history. Thus, we have taken the approach of scaling the relative fluxes by different authors' modern flux estimates (Table 1). In doing so, we find that all authors' frameworks imply an imbalance in Earth's early carbon cycle, with  $C_{total\_input}$  exceeding  $C_{total\_burial}$  (Figure 6).

The most widely accepted models of carbon outgassing and weathering through time invoke higher-than-modern input of carbon to the surface reservoir, whereas the consensus of low Precambrian NPP and near-modern (or lower)  $f_{org}$  implies muted carbon burial. As noted at the outset of the paper, such an imbalance cannot have persisted on geological timescales (Berner & Caldeira, 1997). Thus, some of the accounting detailed above must be incorrect. To consolidate our assessment, we combine Equations 1–4, 9, 10, and 12 to obtain the expanded mass balance expression

$$C_{mantle\_outgassing} + C_{metamorphic\_outgassing} + C_{carb\_weathering} + C_{org\_weathering} = \frac{NPP \times \epsilon_b}{f_{org}} \quad (13)$$

In the rest of the paper, we evaluate the assumptions underlying the estimation of each of these terms in order to determine the most plausible reconciliation of the early Earth's carbon budget.

**Table 1**  
Published Estimates of Fluxes in the Modern Carbon Cycle

References	$C_{\text{carb\_burial}}^{\text{modern}}$	$C_{\text{org\_weathering}}^{\text{modern}}$	$C_{\text{total\_weathering}}^{\text{modern}}$	$C_{\text{mantle\_outgassing}}^{\text{modern}}$	$C_{\text{metamorphic\_outgassing}}^{\text{modern}}$	$C_{\text{total\_outgassing}}^{\text{modern}}$	$C_{\text{total\_input}}^{\text{modern}}$	$f_{\text{org}}$	$C_{\text{org\_burial}}^{\text{modern}}$	$C_{\text{carb\_burial}}^{\text{modern}}$	$C_{\text{total\_burial}}^{\text{modern}}$
Catling and Kasting (2017)	24	7.5 ± 1.7	31.5 ± 1.7	6.5 ± 2.5	2 ± 1	8.5 ± 3.5	40 ± 5.2	0.25	10 ± 1.3	30 ± 3.9	40 ± 5.2
Holland (1978, 1984, 2002, 2009)	39.5	7.5 ± 2.5	47 ± 2.5			3	50 ± 2.5	0.2	10 ± 0.5	40 ± 2	50 ± 2.5
Berner (1991, 2004) [GEOCARB]			18			7	25	0.2	5	20	25
Lenton et al. (2018) [COPSE]	8	3.75 (+4)	11.75 (+4)			16.25	28 (+4)	0.2	5	20	28 <sup>a</sup>
Lee et al. (2016)	20	5	25	4.25 ± 3.25	2.25 ± 0.75	6.5 ± 4.0	31.5 ± 4.0	0.2	6.3 ± 0.8	25.2 ± 3.2	31.5 ± 4.0
This study	14.7 ± 6.2	6.3 ± 2.3	21 ± 8.5	5.1 ± 1.8	2.2 ± 0.7	7.3 ± 2.5	28.2 ± 11.0	0.25	7.1 ± 2.8	21.2 ± 8.3	28.2 ± 11.0

Note. All fluxes are Tmol C/yr. Italics denote numbers that were calculated by assuming the mass balance relationships apply as formulated in Equations 1–4, 9, and 10. Input flux estimates for this study represent the mean (±1σ) of a larger compilation of published estimates (supporting information). In order to guarantee mass balance in our modern parameterization, burial fluxes for this study were calculated using  $C_{\text{total\_input}}$  and  $f_{\text{org}}$ . The values obtained via this method agree well with our literature compilation (supporting information).

<sup>a</sup>Lenton et al. (2018) include a 3 Tmol C/yr removal flux of carbon in basalt alteration, which is not shown in this table.

### 3. Were Carbon Inputs Really Higher in the Precambrian Than Today?

#### 3.1. Carbon Outgassing

One possible solution to the imbalance in the early Earth's carbon budget is that volcanic carbon inputs to the Earth's surface were in fact lower than shown in Figures 1b and 2b. Let us first consider  $C_{\text{mantle\_outgassing}}$ . This term predominantly depends on the secular evolution of heat flow across Earth's history, which is a matter of debate. As shown in Figure 1a, models range from heat flow several times higher in the early Archean (Davies, 2009; Godderis & Veizer, 2000; Sleep & Zahnle, 2001) to near-modern (Korenaga, 2006, 2009).

The lack of consensus surrounding models of early tectonic evolution implies little theoretical basis on which to favor one scenario over the other. So instead, we can consider geologic constraints. Empirical evidence—in the form of Xe isotope systematics of fluid inclusions (Avicé et al., 2017)—has been used to reconstruct relative mantle outgassing rates, yielding an estimate of  $8.1 \pm 3.9$  (1σ) times the modern flux at 3.3 Ga. This is at the upper end of our calculated range of  $R_{\text{mantle\_outgassing}}$  values (Figure 1b), lending credence to the notion of elevated heat flow and carbon outgassing on the early Earth. A more recent study by Marty et al. (2019) modeled Xe isotope evolution and invoked even higher Archean outgassing rates (10–1,000 times modern). If correct, this would mean that even our upper limit underestimates mantle outgassing, further worsening the paradox. Thus, the limited empirical data seem to suggest that lower-than-modern mantle outgassing rates in Earth's early history are unlikely.

In contrast,  $C_{\text{metamorphic\_outgassing}}$  is more difficult to assess, both theoretically and empirically. Some authors have argued that a smaller crustal carbon reservoir would have led to less metamorphic outgassing early in Earth's history (Holland, 2009; Lee et al., 2016). While plausible, it is difficult to quantify the growth of the crustal carbon reservoir through time. Additionally, the relationship between heat flow and metamorphic outgassing is less direct than for mantle outgassing. However, we note that because metamorphic outgassing is likely smaller than the mantle outgassing flux (Table 1)—and the mantle outgassing rate was likely considerably higher in Earth's early history (see above)—removing the metamorphic component from our calculations would not change our conclusions. Inputs would still exceed burial.

In addition to individually reconstructing the component fluxes, here we seek to derive a novel “top-down” constraint on the plausible range for  $C_{\text{total\_outgassing}}$  by assessing the climatic feasibility of different carbon outgassing fluxes. Since the Sun was fainter in its early history (Gough, 1981), elevated CO<sub>2</sub> (and/or CH<sub>4</sub>) levels were likely required to keep the planet warm enough to explain the geological evidence for liquid surface water extending back through nearly all of Earth's history (Feulner, 2012; Sagan & Mullen, 1972). Maintaining high  $p\text{CO}_2$  requires a sufficiently large flux of carbon to the surface reservoir. This is evident in the recent carbon cycle modeling of Krissansen-Totton et al. (2018), which requires higher-than-modern rates of carbon outgassing to maintain warm surface temperatures in the Archean.

Here, we have compiled outputs from the model of Krissansen-Totton et al. (2018) for 3.3 Ga and plotted the global mean surface temperature as a function of total carbon outgassing (Figure 7). The diagram shows that at modern or lower-than-modern outgassing rates, most model runs result in a global mean temperature that is much colder than today, implying widespread glaciation for which there is not geologic evidence. Thus, in order to maintain surface temperatures at

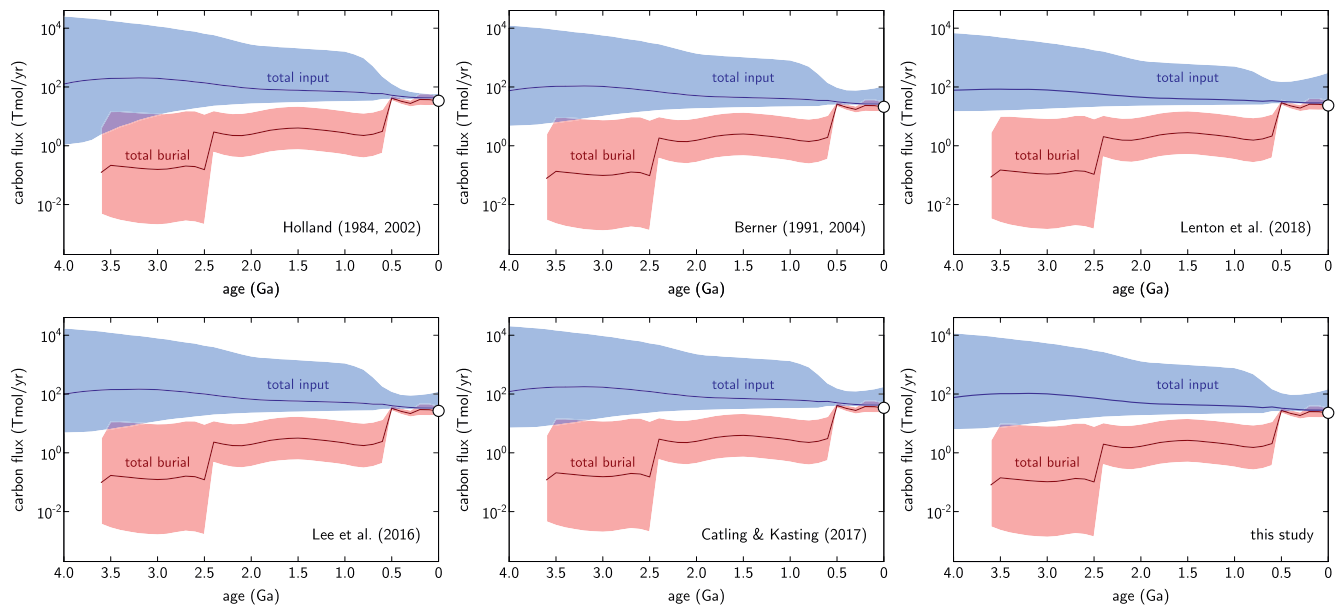


**Figure 6.** The early Earth productivity paradox. Estimates of  $C_{\text{total\_input}}$  exceed those of  $C_{\text{total\_burial}}$ , which cannot be true on geological timescales. Total input fluxes were compiled from Figures 1b, 2b, 3d, and 4b; total burial fluxes were compiled from Figures 5b and 5d. Relative fluxes were scaled to modern values using different authors' frameworks, as shown in Table 1. In all cases, carbon input significantly exceeds carbon burial in Earth's early history.

3.3 Ga that are consistent with proxy evidence and modeling results (e.g., Figure 3b), rates of carbon outgassing likely needed to be several times the modern flux (Figure 7).

Considering all of the evidence above, we find it unlikely that volcanic carbon fluxes to the Earth's surface were lower in the Precambrian than they are today. If anything, outgassing was likely higher, as suggested by Xe isotope systematics in Archean kerogen. Furthermore, carbon cycle modeling suggests that high carbon outgassing rates are required to explain the lack of evidence for large-scale glaciation in the mid-Archean.

### 3.2. Carbon Weathering

If carbon outgassing was proceeding more rapidly in Earth's early history, perhaps the paradox can still be resolved if weathering inputs of carbon were substantially lower than modern. Let us first consider  $C_{\text{org\_weathering}}$ . The rate of organic carbon weathering depends on  $p\text{O}_2$ , though exactly how these terms are related remains debated (Bolton et al., 2006; Daines et al., 2017; Derry, 2014). Our  $C_{\text{org\_weathering}}$  calculation invoked an  $\text{O}_2$  dependence of  $p\text{O}_2^{0.5}$  (cf., Chang & Berner, 1999; Daines et al., 2017; Lasaga & Ohmoto, 2002). This leads to substantially lower  $C_{\text{org\_weathering}}$  in the Proterozoic, and negligible rates in the Archean (Figure 4b). At these levels, organic weathering is unimportant. If anything, the true  $\text{O}_2$ -dependence of organic weathering is slightly weaker than we have assumed because thermogenic methane, which is part of the organic weathering flux (Derry, 2014), will be oxidized to  $\text{CO}_2$  even under low- $\text{O}_2$  conditions (and thus could still oxidize organic matter effectively in the Precambrian). This means that if anything the paradox is slightly worse than we have calculated (i.e., inputs would be higher in the Archean). Thus, we find that uncertainty surrounding the reconstruction of  $C_{\text{org\_weathering}}$  likely cannot resolve the paradox.

Next we consider  $C_{\text{carb\_weathering}}$ . To a first order, carbonate weathering is sensitive to the amount of carbonate exposed to weathering on land. We have considered a wide range of histories for continental landmass (Figure 3a), and even under the scenario that invokes the slowest growth of emerged continents, the carbonate weathering flux is only negligible in the early Archean (Figure 3d). The heightened carbonate weathering fluxes calculated for much of the Precambrian derive mainly from the elevated  $p\text{CO}_2$  required to keep the Earth warm under weaker solar luminosity (Figure 3c). Thus, despite the possibility of less-than-modern emergent landmass, Precambrian carbonate weathering fluxes are likely to have been similar to modern rates or higher.

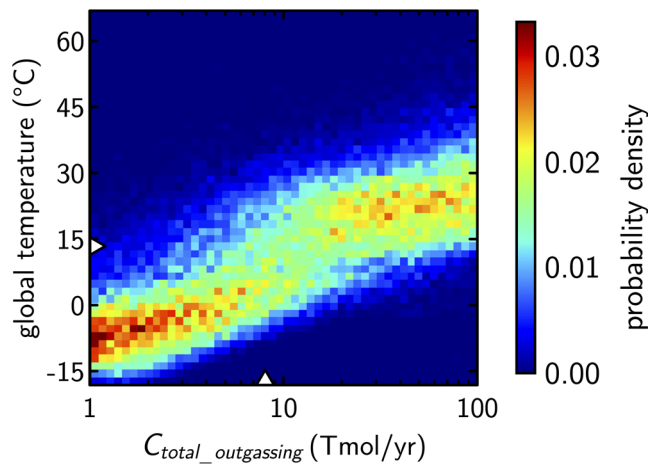


**Figure 7.** Global mean temperature as a function of total carbon outgassing. Results compiled from nominal model of Krissansen-Totton et al. (2018) at 3.3 Ga. For each assumed outgassing flux, the heatmap shows the likely distribution of mean surface temperatures given uncertainties in carbon cycle evolution. White triangles denote modern temperature and the approximate modern outgassing flux. If Archean outgassing was significantly less than the modern flux, then the model predicts Earth would have been extensively glaciated, contrary to geologic evidence. This supports empirical Xe isotope constraints and heat flow arguments for Precambrian outgassing being comparable to or greater than modern outgassing. Thus, the productivity paradox probably cannot be resolved by low Precambrian outgassing.

While the majority of acceptable parameter space invokes higher carbonate weathering in deep time, this is by far the most uncertain input flux, with end-member estimates spanning many orders of magnitude. Despite this uncertainty, we note that even taking the extreme assumption that Archean continents were entirely submerged (Flament et al., 2008)—which would eliminate both the organic and carbonate weathering fluxes (i.e.,  $f_{\text{land}} = 0$ )—the empirically constrained mid-Archean mantle outgassing rates ( $8.1 \pm 3.9$  times the modern rate; Avicé et al., 2017) alone are higher than the coeval upper limits on  $C_{\text{total\_burial}}$  as calculated in Figure 6. Thus, we find that even with considerable uncertainty surrounding the determination of carbon input fluxes to the Earth's surface through time, it is unlikely that invoking a lower rate of total carbon input is a valid solution to the productivity paradox.

## 4. Was Carbon Burial Really Lower in the Precambrian Than Today?

### 4.1. Fractional Organic Carbon Burial and the Carbon Isotope Record

The balance of evidence reviewed in Section 3 suggests that  $C_{\text{total\_input}}$  was likely higher in Earth's early history than it is today, with the lowest plausible estimates falling near modern values (Figure 6). This means that in order to explain mass balance in the early carbon cycle,  $C_{\text{total\_burial}}$  must have been higher than was suggested in the accounting of Section 2. Considering the right-hand side of Equation 13, there are three terms that we can manipulate in order to change the burial rate: NPP,  $\epsilon_b$ , and  $f_{\text{org}}$ .

We begin with  $f_{\text{org}}$ . One way to resolve the paradox would be to shrink the denominator in Equation 13, thereby boosting total burial rates. Some authors have indeed argued that the canonical interpretation of the  $\delta^{13}\text{C}$  record (i.e., the framework of Equation 11, which was used to the  $f_{\text{org}}$  trend shown in Figure 5c) is invalid for the Precambrian, in other words suggesting that  $\delta^{13}\text{C}_{\text{carb}}$  and  $\delta^{13}\text{C}_{\text{org}}$  were decoupled from fractional organic burial. This would allow for the possibility that we are overestimating  $f_{\text{org}}$ , and therefore underestimating  $C_{\text{total\_burial}}$ . Broadly speaking, these hypotheses can be divided into (i) missing sink hypotheses and (ii) variable  $\delta^{13}\text{C}_{\text{input}}$  hypotheses.

Bjerrum and Canfield (2004) proposed a missing sink whereby the canonical view of carbon isotope mass balance neglects seafloor weathering (i.e., precipitation of carbonate in seafloor basalts), which may have been important in the Archean. High concentrations of carbonate in Archean basalts seem to support this hypothesis (Nakamura & Kato, 2004). However, in this model an isotopic gradient between surface and deep waters is needed to reconcile the  $\delta^{13}\text{C}$  record with lower Archean  $f_{\text{org}}$ . Such an isotopic offset between seafloor and continental carbonates is not observed (Krissansen-Totton et al., 2015; Nakamura & Kato, 2004), although the preserved basalts may not be representative of the Archean oceanic crust, which has been largely subducted.

Schrag et al. (2013) argued for another missing sink: a sizable authigenic carbonate sink that is neglected in the canonical mass balance. This omission of isotopically light carbonates could, in principle, allow for lower “true” Precambrian  $f_{\text{org}}$ , although there is limited direct evidence for such a sink. Krissansen-Totton et al. (2015) presented calculations reconstructing  $f_{\text{org}}$  over Earth history allowing for both a missing seafloor weathering sink and a missing authigenic carbonate sink. They found that the inclusion of these missing sinks only enabled a relative change in  $f_{\text{org}}$  over Earth's history less than a factor of 1.4 ( $+15^{+140}_{-71}\%$  increase; 95% confidence), which alone cannot reconcile the observed imbalance between carbon inputs and outputs.

An alternative explanation for decoupling the  $\delta^{13}\text{C}$  record from  $f_{\text{org}}$  is varying the  $\delta^{13}\text{C}$  value of carbon inputs. When estimating  $f_{\text{org}}$  through time,  $\delta^{13}\text{C}_{\text{input}}$  is typically assumed to equal mantle values throughout Earth's history. Indeed, peridotitic xenoliths, mantle-derived basalts, and carbonatites all suggest that the  $\delta^{13}\text{C}$  of

the upper mantle has remained unchanged throughout Earth's history (Holser & Schidlowski, 1988; Matthey, 1987; Pearson et al., 2014). However, the  $\delta^{13}\text{C}$  value of carbon inputs into the atmosphere-ocean system is the weighted sum of mantle outgassing, metamorphic outgassing, and contribution from the weathering carbonates and organics, the latter of which includes thermogenic methane. Recognizing this, Derry (2014) argued that under reducing Precambrian conditions, the incomplete oxidation of organic matter may have resulted in elevated  $\delta^{13}\text{C}_{\text{input}}$  (due to a lower contribution from isotopically light organic weathering).

If  $\delta^{13}\text{C}_{\text{input}}$  was in fact higher in the Precambrian, it would imply that the “true”  $f_{\text{org}}$  was lower than we have typically inferred (Equation 11). This was further investigated by Daines et al. (2017), who incorporated  $\text{O}_2$ -dependent organic weathering into a carbon-oxygen cycle model to show how changes in  $f_{\text{org}}$  may not be reflected in the carbonate  $\delta^{13}\text{C}$  record because  $\delta^{13}\text{C}_{\text{input}}$  is changing. Their study was focused on organic weathering *after* the GOE, since weathering of sedimentary organic matter is negligible at pre-GOE oxygen levels (as discussed in Section 3.2). Thus, this mechanism could not have induced carbon isotope excursions in the Archean, when the productivity paradox was most pronounced (Figure 6). Furthermore, the model of Daines et al. did not track the secular isotopic evolution of crustal carbon reservoirs, meaning that their results potentially imply a trajectory in the  $\delta^{13}\text{C}$  of crustal carbon that is inconsistent with the rock record. For these reasons, invoking lower “true”  $f_{\text{org}}$  in the Precambrian does not seem to be a valid solution to the early Earth's carbon budget imbalance.

In sum, while uncertainty surrounds reconstructions of  $f_{\text{org}}$  from the  $\delta^{13}\text{C}$  record, none of the hypotheses for decoupling of  $f_{\text{org}}$  and  $\delta^{13}\text{C}$  can readily explain a low enough “true”  $f_{\text{org}}$  value to account for the apparent imbalance in the early carbon budget. Thus, given the existing empirical constraints, this effect cannot resolve the early Earth productivity paradox.

#### 4.2. Net Primary Productivity

Moving next to the numerator on the right-hand side of Equation 13, we can consider constraints on NPP in the Precambrian. There are various theoretical arguments that have been put forth invoking lower NPP in the early biosphere. Prior to the evolution of oxygenic photosynthesis, it is likely that NPP was limited by the supply of reductants (e.g.,  $\text{H}_2$ ,  $\text{Fe}^{2+}$ , and  $\text{H}_2\text{S}$ ) to primary producers (Canfield et al., 2006; Kharecha et al., 2005; Ward et al., 2019). Estimated annual fluxes for these electron donors are highly uncertain, though studies agree that even the most extreme plausible fluxes would support NPP at rates 1–2 orders of magnitude lower than today (Canfield et al., 2006; Kharecha et al., 2005; Ward et al., 2019) (Figure 5a). Thus, we find no reason to suspect that before the evolution of oxygenic photosynthesis, NPP could have approached the levels necessary to balance estimated carbon inputs. However, if oxygenic photosynthesis arose very early in Earth's history (perhaps  $>3.8$  Ga, reviewed in Buick, 2008), this upper limit may not apply for much of the Archean.

Following the evolution of oxygenic photosynthesis, with water acting as a ubiquitous electron donor, it is likely that macronutrients came to set the limit on NPP. Phosphorus (P) is typically thought to be the rate-limiting reactant for NPP on geological timescales, because nitrogen can be fixed from atmospheric  $\text{N}_2$  when it is scarce (Tyrrell, 1999). Thus, most work aimed at evaluating NPP after the rise of oxygenic photosynthesis has focused on reconstructing marine P levels.

Early on, Bjerrum and Canfield (2002) suggested that in the Fe-rich Precambrian ocean, P may have been scavenged onto Fe oxides and transported to sediments, thus choking off the supply of P to primary producers via an “Fe trap.” This pathway operates in the modern ocean (Berner, 1973), lending credence to the hypothesis. Furthermore, the P/Fe ratio in modern Fe-scavenging systems (i.e., proximal to hydrothermal Fe input) correlates with dissolved P levels (Feely et al., 1998), thus providing a way to leverage Fe-rich marine sedimentary rocks to quantify dissolved P levels in deep time. In their seminal paper, Bjerrum and Canfield (2002) found low P/Fe ratios in Archean and early Paleoproterozoic banded iron formations, which they interpreted as evidence of dissolved P concentrations that were 10%–25% of modern levels. In the simplest view of P-limited NPP, this would imply proportionally lower NPP in the Archean ocean (i.e., 10%–25% of modern NPP; Figure 5a).

Since that pioneering study, there have been considerable revisions to the “Fe-trap” hypothesis for Precambrian P limitation. First, Konhauser et al. (2007) showed that competing adsorption of Si onto Fe-oxides

would lead to lower P/Fe for a given P concentration, meaning that the P/Fe ratios observed by Bjerrum and Canfield (2002) could potentially be consistent with *higher-than-modern* dissolved P levels under plausible estimates of marine [Si] (up to ~2.2 mM) prior to the evolution of siliceous planktonic primary producers. Jones et al. (2015) took cation competition a step further, incorporating  $Mg^{2+}$  and  $Ca^{2+}$  into a model of Fe-scavenging in the Precambrian ocean, and concluded that despite competing adsorption by other species, the low P/Fe ratios in Archean and early Paleoproterozoic BIFs most likely reflected low dissolved P (<20% modern levels). Thus, in light of that work, the picture remained one of low P (and NPP) due to Fe-scavenging.

More recently, in part motivated by studies suggesting that reduced or mixed-valence Fe minerals played an important role in the genesis of iron formations (e.g., Rasmussen et al., 2013, 2015), some authors have suggested that instead of Fe-oxides, vivianite (Derry, 2015) or green rust (Halevy et al., 2017) could have dominated P scavenging from the Precambrian water column. In principle, the valence state of the Fe mineral scavenging P is unimportant so long as P is indeed scavenged, though it does complicate the quantitative relationship between P/Fe in BIFs (which is calibrated based on adsorption to Fe-oxides in the modern ocean; Feely et al., 1998) and dissolved P levels at the time of deposition. Reinhard et al. (2017b) recently provided a new perspective on this issue, compiling P concentrations in marginal marine siliciclastic marine sediments through Earth's history, and found that P burial was muted (~4× lower on average) prior to the late Neoproterozoic. They incorporated the latest views of Fe scavenging by multiple Fe minerals into a model of marine P cycling, finding that their data could be explained by Fe scavenging via reduced or mixed-valence Fe minerals, resulting in a low-P ocean. So, despite revision of mechanistic underpinnings, the prevailing view remains one of low P (and NPP) due to Fe-scavenging.

In contrast to the predominant view of an “Fe-trap” limiting Precambrian P levels, an alternative mechanism has been proposed for P limitation: limited recycling of organic matter (and associated P) in an oxidant-poor ocean (Kipp & Stüeken, 2017). In this model, an “Fe-trap” is not needed to achieve low marine P levels; rather, P is rapidly utilized by primary producers upon riverine input to the ocean, and then efficiently buried with organic matter exported to marine sediments. Thus, the regeneration of P—which in the modern ocean sustains a large P reservoir with a long marine residence time (Schlesinger & Bernhardt, 2013)—would have been muted, keeping marine P levels low. Such a mechanism was also invoked by Laakso and Schrag (2018) in the context of the Proterozoic ocean specifically, suggesting that limited P recycling could have served as the dominant control on P levels through most of the Precambrian, rather than Fe scavenging. Despite invoking a different mechanism than the “Fe-trap” hypothesis, the “limited recycling” model also implies P levels (and NPP) in the Precambrian ocean that are substantially lower than modern (<<40% modern P levels in the Archean; Kipp & Stüeken, 2017). So, whether limited P recycling or Fe-scavenging (or both) controlled P levels during the Precambrian, all models point to lower-than-modern P (and accordingly, NPP).

One complication of using inferred marine P levels to constrain NPP in deep time is that it requires an assumption about the C:P ratio of primary producers. While today this ratio is fairly conserved across the ocean (~106; Redfield, 1958), it is known that under severe nutrient scarcity cyanobacteria can grow with C:P ratios of ~300 or higher (e.g., White et al., 2006). This has led some authors to infer that the average C:P ratio of primary producers in the Precambrian ocean was much higher than at present (e.g., Reinhard et al., 2017). A higher C:P ratio would mean that NPP (which is defined as a carbon fixation flux) could have been higher than we have inferred from assuming direct proportionality to P levels. To address this possibility, we have considered a case where C:P = 400 (cf., Reinhard et al., 2017). In this scenario, the increase in total carbon burial (~4× higher) is still far too small to balance carbon inputs (Figure S1). We therefore conclude that variable phytoplankton stoichiometry is an insufficient solution to the productivity paradox, though we note it may play a role and at present remains poorly constrained.

While theoretical and empirical records support low P (and NPP) in the Precambrian, is there a more direct archive of NPP in deep time? Recent work has aimed to leverage rare oxygen isotope anomalies ( $\Delta^{17}O$ ) in sulfate minerals as such an archive, following early work by Luz et al. (1999). For given environmental parameters (e.g.,  $pO_2$  and  $pCO_2$ ), the magnitude of these anomalies is a function of biospheric  $O_2$  production, which can be equated to gross primary production (GPP) more readily than NPP (Luz et al., 1999). The difference between GPP and NPP is the respiration conducted by primary producers (Sigman & Hain, 2012);

NPP/GPP ratios are somewhat variable in the modern ocean, and may have varied through Earth's history under different environmental conditions. While this variability introduces uncertainty to NPP estimates derived from  $\Delta^{17}\text{O}$ , here we take the simple assumption that the NPP/GPP ratio has remained unchanged in order to get a first-order estimate of NPP based on the sulfate  $\Delta^{17}\text{O}$  record. Recent measurements of  $\Delta^{17}\text{O}$  in Precambrian barites (Crockford et al., 2018; Hodgskiss et al., 2019) imply GPP of well below half of modern levels in the mid-Proterozoic, with potentially higher values in the Paleoproterozoic, though these estimates are confounded by uncertainty in  $p\text{O}_2$  reconstructions at that time. While not a precise record of NPP, we take these results as consistent with the P-based lines of reasoning for lower NPP (likely well below half of modern levels, perhaps closer to  $\sim 10\%$  modern) during most of the Precambrian.

In sum, a variety of theoretical and empirical arguments suggest lower NPP during the Precambrian. While distinguishing between particular mechanisms has proven challenging, models suggest that NPP could have been lower than modern levels by an order of magnitude or more. Perhaps most telling is that arguments for higher-than-modern NPP are lacking in the literature. Thus, we find that invoking high NPP is an implausible solution to the paradox.

## 5. High Burial Efficiency as a Solution to the Paradox

### 5.1. Satisfying C Cycle Mass Balance With High Burial Efficiency

We now have a single remaining variable with which to remedy the paradox of carbon cycle imbalance in Earth's early history:  $\varepsilon_b$ . Higher  $\varepsilon_b$  would allow greater carbon burial despite limited NPP and near-modern  $f_{\text{org}}$ . Is this plausible?

Using our  $C_{\text{org\_burial}}^{\text{modern}}$  estimate of 7.1 Tmol C/yr (Table 1) and an  $\text{NPP}^{\text{modern}}$  estimate of 4,000 Tmol C/yr (Field et al., 1998), we obtain an  $\varepsilon_b^{\text{modern}}$  value of  $\sim 0.2\%$ , which agrees well with other authors' estimations of modern burial efficiency ( $\sim 0.3\%$ , Holland, 1978;  $< 0.5\%$ , Hedges & Keil, 1995;  $\sim 0.2\%$ , Laakso & Schrag, 2018;  $\sim 0.5\%$ , Middelburg, 2019). However, in modern anoxic settings,  $\varepsilon_b$  is known to be higher than the globally averaged value (Hedges & Keil, 1995). For instance,  $\varepsilon_b$  has been estimated at 1–3% in the Black Sea (Arthur et al., 1994), which has oxygen-depleted bottom waters and appreciable dissolved  $\text{H}_2\text{S}$ —similar to conditions that are thought to have prevailed, at least periodically, in the late Archean and Proterozoic oceans (Canfield, 1998; Poulton et al., 2004; Scott et al., 2011). Perhaps a better analog for the Archean ocean is the anoxic, low-sulfate Lake Matano, which features  $\varepsilon_b$  as high as 20–60% (Kuntz et al., 2015). While the physiographic and sedimentological properties of Lake Matano are different from those of the global ocean, which could impact the degree to which this is a fully appropriate analog for global burial efficiency, the lake shows that a high proportion of exported organic matter can in fact be buried when the oxidants needed to fuel remineralization are in short supply.

Is this a reasonable scenario to invoke for the Precambrian ocean at large? As noted in Section 4, previous work has already suggested high burial efficiency by calculating the stoichiometric capacity for remineralization in the oxidant-poor Archean and Proterozoic oceans (Kipp & Stüeken, 2017). That work demonstrated that oxidant scarcity could have inhibited organic remineralization (i.e., increased burial efficiency), which would have resulted in lower P recycling and thus low steady-state marine P levels. But could  $\varepsilon_b$  have been high enough to balance the high carbon inputs suggested in Section 3?

We used the right-hand side of Equation 13 to determine the increase in  $\varepsilon_b$  required to balance carbon inputs and outputs through Earth history. The contours in Figure 8a denote the total carbon burial flux for different values of  $\varepsilon_b$ , assuming that the upper limit on NPP (top of the shaded region in Figure 5a) is correct. If these NPP estimates are accurate, then  $\varepsilon_b$  would need to be in the few percent to tens of percent range to balance the modeled carbon inputs (Figure 8a). This spans the range of  $\varepsilon_b$  observed in modern reducing settings (Black Sea and Lake Matano), suggesting that it is plausible to invoke such high burial efficiency in the Precambrian ocean. However, if NPP was in fact much lower than the upper limit, then  $\varepsilon_b$  would need to be correspondingly higher.

Based on the calculations shown in Figure 8a, NPP levels 1–2 orders of magnitude lower than the upper limit in Figure 5a could still potentially be reconciled with carbon inputs (so long as the actual input rate

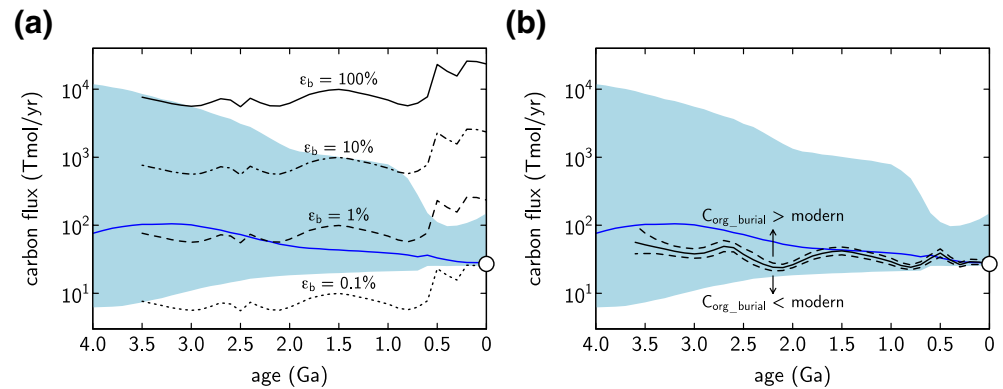


**Figure 8.** High burial efficiency as a solution to the productivity paradox. In both panels, the blue shaded region denotes plausible range of  $C_{\text{total\_burial}}$  as shown in Figure 6f and the white circle denotes modern values. In panel (a), contours denote  $C_{\text{total\_burial}}$  for given values of  $\epsilon_b$ . Calculations utilized the upper limit on NPP as shown in Figure 5a. In panel (b),  $\epsilon_b$  is assumed to increase as much as needed to balance carbon inputs and outputs; the solid line then denotes a contour where the implied  $C_{\text{org\_burial}}$  flux equals the modern rate. This is calculated using Equation 10 and the  $f_{\text{org}}$  trajectory of Krissansen-Totton et al. (2015) (Figure 5c).

was near the middle of our calculated uncertainty range). However, if NPP was 3 orders of magnitude lower than the upper limit, as suggested by Ward et al. (2019) for the Archean (Figure 5a), then it could be impossible to balance carbon inputs and burial, even with 100% burial efficiency. Such extremely low NPP therefore seems unlikely in light of these calculations, though we note that it is difficult to definitively rule out any scenario given the uncertainty in all flux estimates. In any case, plausible NPP estimates and  $\epsilon_b$  values that match those of modern reducing environments are able to match the high carbon input rates inferred for the Archean.

So is the paradox solved? Plausible increases in  $\epsilon_b$  can readily explain mass balance in the early carbon cycle, and such increases are in fact expected due to the scarcity of oxidants in the Precambrian ocean. Invoking higher  $\epsilon_b$  thus resolves the imbalance by allow higher  $C_{\text{total\_burial}}$  in spite of low NPP. Specifically, this happens by enabling substantial organic carbon burial, potentially at rates exceeding the modern flux (Figure 8b). From the perspective of carbon cycle mass balance, this is perfectly acceptable. However, by invoking substantial organic carbon burial, we may be creating a problem with the Archean redox budget.

Ever since the rise of oxygenic photosynthesis, every mole of buried organic carbon has equated to a mole of O<sub>2</sub> accumulated at Earth's surface (and before that, some other oxidized species). It is well established that  $p\text{O}_2$  remained vanishingly low ( $<10^{-6}$  times the present atmospheric value; Catling & Zahnle, 2020; Farquhar et al., 2000; Pavlov & Kasting, 2002; Zahnle et al., 2006) prior to the GOE at ~2.4 Ga (Gumsley et al., 2017; Warke et al., 2020). Thus, if we are to invoke high burial efficiency as a solution to the early Earth productivity paradox, we must ensure that such a scenario is consistent with a low-O<sub>2</sub> Archean atmosphere.

## 5.2. Satisfying the Archean Redox Budget With High Burial Efficiency

We follow the approach of Claire et al. (2006), Kasting (2013), and Kadoya et al. (2020b) by using the parameter  $K_{\text{OXY}}$  to assess the redox balance of the Archean atmosphere. The parameter is defined as the balance between O<sub>2</sub> sources and kinetically rapid sinks (i.e., not oxidative weathering, which is only significant at  $p\text{O}_2$  orders of magnitude higher than Archean values), such that

$$K_{\text{OXY}} = \frac{F_{\text{org\_burial}} + F_{\text{FeS}_2\text{burial}}}{F_{\text{reduced outgassing}}} \quad (14)$$

Here, each flux term is expressed in terms of O<sub>2</sub> equivalents, which is identical to carbon assuming a 1:1 C:O<sub>2</sub> net stoichiometry of organic burial. While the O<sub>2</sub>:C stoichiometry of phytoplankton anabolism and heterotrophic respiration is fairly constant in the modern ocean (Anderson & Sarmiento, 1994; Tanioka &

Matsumoto, 2020), this ratio in theory could have fluctuated across Earth's history as the molecular composition of primary producers evolved. However, the C:O<sub>2</sub> stoichiometry of respiration for individual components of phytoplankton biomass suggests that such changes would be relatively small ( $\pm 25\%$ ), similar in magnitude to the uncertainty in our  $K_{\text{Oxy}}$  calculation deriving from the flux estimates (see below). We therefore note that while this might be an additional knob to tune in order to precisely assess Archean redox balance, at present it is too uncertain and too small in magnitude to warrant further treatment.

The parameter works as follows: when  $K_{\text{OXY}} < 1$ , the kinetically efficient O<sub>2</sub> sink of oxidizable gases exceeds oxygen sources, and the atmosphere is anoxic; thus, excess hydrogen builds up in the atmosphere and escapes to space. Note that hydrogen escape is excluded by design in the numerator of  $K_{\text{OXY}}$  to make  $K_{\text{OXY}} < 1$ . When  $K_{\text{OXY}}$  exceeds unity, oxygen sources outweigh the oxygen sink of oxidizable gases; hence, O<sub>2</sub> builds up in the atmosphere and is consumed by oxidative weathering (i.e., the GOE occurs). Note that oxidative weathering is excluded by design in the denominator of  $K_{\text{OXY}}$  to make  $K_{\text{OXY}} > 1$  under such oxygenated circumstances.

The carbon-related terms are calculated as

$$F_{\text{org\_burial}} = f_{\text{org}} (C_{\text{total\_outgassing}} + C_{\text{total\_weathering}}) \quad (15)$$

$$F_{\text{reduced\_outgassing}} = \left( \frac{C_{\text{total\_outgassing}}}{C_{\text{total\_outgassing}}^{\text{modern}}} \right) F_{\text{reduced\_outgassing}}^{\text{modern}} \quad (16)$$

Where the O<sub>2</sub> production derived from organic carbon burial ( $F_{\text{org\_burial}}$ ) (which here is the stoichiometric equivalent of  $C_{\text{org\_burial}}$ ) is calculated by multiplying total inputs by  $f_{\text{org}}$ . The calculation of O<sub>2</sub> consumption, ( $F_{\text{reduced\_outgassing}}$ ; Equation 16), allows the outgassing flux of reductants to scale with changes in the carbon outgassing rate. For the reduced sulfur burial term ( $F_{\text{FeS}_2\text{burial}}$ ), we utilize estimates from the literature (see below).

Kasting (2013) gives a thorough discussion of the uncertainties on each flux in this calculation. Despite these uncertainties, the literature surrounding each piece of this redox puzzle is sufficiently mature that most recently published values are of similar magnitude. Furthermore, we do not seek here to precisely capture the redox threshold across which the GOE was initiated or to precisely define the redox balance of the Archean atmosphere. Rather, we merely aim to demonstrate whether high burial efficiency can plausibly be invoked as a solution to the productivity paradox while maintaining an anoxic Archean atmosphere.

First, we demonstrate that the equation properly describes modern redox balance. Using modern parameter values (Table 2) we obtain a  $K_{\text{OXY}}$  value of  $5.0 \pm 1.1$ . This gives a decidedly oxic atmosphere and is fairly close to previous formulations (Claire et al., 2006; Kasting, 2013; Krissansen-Totton et al., 2015), though is slightly lower (previous estimates are  $\sim 6$ ) because we have included more recent estimates of  $C_{\text{carb\_weathering}}$  that are lower than was suggested in earlier work. Thus, we note that if anything, this accounting might make it slightly easier to achieve anoxia in the Archean atmosphere.

Next, we can modify the equation to describe Archean redox balance. We start by extracting  $f_{\text{org}}$  from the carbon isotope record, which at 3.3 Ga gives a value of 0.15 (Krissansen-Totton et al., 2015). To obtain net organic burial, we must multiply  $f_{\text{org}}$  by total carbon inputs. Because high burial efficiency can potentially account for organic carbon burial in excess of net carbon inputs (Figure 8a), we need not worry about NPP estimates here. Instead, we simply explore a range of  $C_{\text{total\_weathering}}$  (1 – 100 Tmol C/yr) and  $C_{\text{total\_outgassing}}$  (1 – 100 Tmol C/yr) fluxes that are much lower and higher than the modern values and span plausible parameter space for 3.3 Ga (Figures 1–4). We then approach the calculation first by leaving all other terms unchanged in order to isolate the effect of burial efficiency.

At first glance, this calculation shows that burying organic carbon at near-modern rates is perhaps problematic for maintaining atmospheric anoxia. Using putative flux estimates for 3.3 Ga and keeping other parameters unchanged (Table 2, Scenario A),  $K_{\text{OXY}}$  is  $1.1^{+0.8}_{-0.3}$  (Figure 9a), which implies an oxygenated atmosphere, inconsistent with proxy data. However, there are a few ways in which this calculation could be modified to become consistent with an anoxic Archean atmosphere. First, following Holland (2002; 2009),

**Table 2**  
Parameter Values Used for  $K_{\text{OXY}}$  Calculations

	Modern	Scenario A	Scenario B	Scenario C	Scenario D
$C_{\text{mantle\_outgassing}}$	$5.1 \pm 1.8$ (Table 1)	$41 \pm 20 [C_{\text{mantle\_outgassing}}^{\text{modern}} \times 8.1 \pm 3.9$ (Avice et al., 2017)]	$41 \pm 20 [C_{\text{mantle\_outgassing}}^{\text{modern}} \times 8.1 \pm 3.9$ (Avice et al., 2017)]	$41 \pm 20 [C_{\text{mantle\_outgassing}}^{\text{modern}} \times 8.1 \pm 3.9$ (Avice et al., 2017)]	$41 \pm 20 [C_{\text{mantle\_outgassing}}^{\text{modern}} \times 8.1 \pm 3.9$ (Avice et al., 2017)]
$C_{\text{metamorphic\_outgassing}}$	$2.2 \pm 0.7$ (Table 1)	0	0	0	0
$C_{\text{carb\_weathering}}$	$14.7 \pm 6.2$ (Table 1)	$24 \pm 10$ (Figure 3d)	$24 \pm 10$ (Figure 3d)	$24 \pm 10$ (Figure 3d)	$24 \pm 10$ (Figure 3d)
$C_{\text{org\_weathering}}$	$6.3 \pm 2.3$ (Table 1)	0	0	0	0
$f_{\text{org}}$	0.25 (Krissansen-Totton et al., 2015)	0.15 (Krissansen-Totton et al., 2015)	0.15 (Krissansen-Totton et al., 2015)	0.15 (Krissansen-Totton et al., 2015)	0.15 (Krissansen-Totton et al., 2015)
$F_{\text{FeS}_2\text{\_burial}}$	5.0 (Holland, 2002)	5.0 (Holland, 2002)	2.5 (Holland, 2002)	2.5 (Holland, 2002)	2.5 (Holland, 2002)
$F_{\text{reduced\_outgassing}}$	2.4 (Holland, 2002)	$13.5 \pm 6.6 [F_{\text{reduced\_outgassing}}^{\text{modern}} \times (C_{\text{total\_outgassing}}^{\text{modern}} / C_{\text{total\_outgassing}}^{\text{modern}})]$	$13.5 \pm 6.6 [F_{\text{reduced\_outgassing}}^{\text{modern}} \times (C_{\text{total\_outgassing}}^{\text{modern}} / C_{\text{total\_outgassing}}^{\text{modern}})]$	$24.3 \pm 11.8 [F_{\text{reduced\_outgassing}}^{\text{modern}} \times (C_{\text{total\_outgassing}}^{\text{modern}} / C_{\text{total\_outgassing}}^{\text{modern}}) \times 1.8]$ ( $f_{\text{O}_2}$ increase of 0.5 log units)	$43.1 \pm 21.0 [F_{\text{reduced\_outgassing}}^{\text{modern}} \times (C_{\text{total\_outgassing}}^{\text{modern}} / C_{\text{total\_outgassing}}^{\text{modern}}) \times 3.2]$ ( $f_{\text{O}_2}$ increase of 1.0 log units)
$K_{\text{OXY}}$	$5.0^{+1.1}_{-1.1}$	$1.1^{+0.8}_{-0.3}$	$0.9^{+0.6}_{-0.2}$	$0.5^{+0.4}_{-0.1}$	$0.3^{+0.2}_{-0.1}$

Note. Fluxes are in Tmol/yr;  $f_{\text{org}}$  and  $K_{\text{OXY}}$  are unitless.

the  $F_{\text{FeS}_2\text{\_burial}}$  term can be adjusted to account for the possibility that volcanic outgassing in the Archean had a higher ratio of  $\text{H}_2$  to  $\text{CO}_2$  and  $\text{SO}_2$  (Table 2, Scenario B). This could suppress pyrite burial by a factor of  $\sim 2$  (Kasting, 2013), which helps to bring  $K_{\text{OXY}}$  down slightly ( $0.9^{+0.6}_{-0.2}$ ), though still leaves plausible Archean fluxes falling near the oxygenation threshold (Figure 9b). Because the Archean atmosphere was persistently anoxic over  $>10^8$  yr timescales,  $K_{\text{OXY}}$  likely needs to be well below unity.

Another possible remedy to this redox problem is that the flux of reduced gases was proportionally greater in the Archean than it is today. In other words,  $F_{\text{reduced\_outgassing}}$  may need to be scaled not just with the relative outgassing rate, but also by some factor that allows for changes in the redox state of outgassed material. A few hypotheses have been put forth that would explain such a scenario.

Some authors have argued that a shift from predominantly submarine to predominantly subaerial volcanism in the late Archean could have shifted the redox state of outgassed material toward a more oxidized composition (e.g., Kump & Barley, 2007; Gaillard et al., 2011). This scenario is difficult to definitively rule out, though there are some unresolved issues that warrant further scrutiny (e.g., Kasting, 2013; Kasting et al., 2012). For instance, the many models invoking fairly rapid continental growth (Figure 3a) may indicate that subaerial volcanism was already prevalent in the Archean. Also, using the  $K_{\text{OXY}}$  approach to evaluate this mechanism reveals that it alone is insufficient to cause the anoxic-oxic transition at the GOE (Kasting, 2013); while it may contribute, additional mechanisms are needed. We therefore note that a shift in the primary locus of volcanism may have been a contributor to Archean redox balance, but consider it unlikely to be the sole solution to the redox problem posed above.

Another hypothesis for a shift in the redox state of outgassed material focuses on the redox state of the upper mantle. Early studies of the trace element content of Archean magmatic rocks suggested that the mantle redox state changed very little through time (Canil, 1997; Li & Lee, 2004; Trail et al., 2011). However, more recent work has used similar methods to invoke a change in mantle redox since the Archean of  $\sim 1$  log unit  $f_{\text{O}_2}$  (Aulbach & Stagno, 2016; Nicklas et al., 2019). If the upper mantle were indeed more reduced,  $F_{\text{reduced\_outgassing}}$  would increase relative to  $F_{\text{org\_burial}}$ , thereby suppressing  $K_{\text{OXY}}$  values (Kadoya et al., 2020b).

Regardless of which mechanism (if any) is most likely, we explore here the effect of enhanced outgassing of reductants in order to determine whether it can resolve the Archean redox budget under high organic burial efficiency. We consider two scenarios: relative increases in  $F_{\text{reduced\_outgassing}}$  of 1.8 and 3.2 (Table 2,

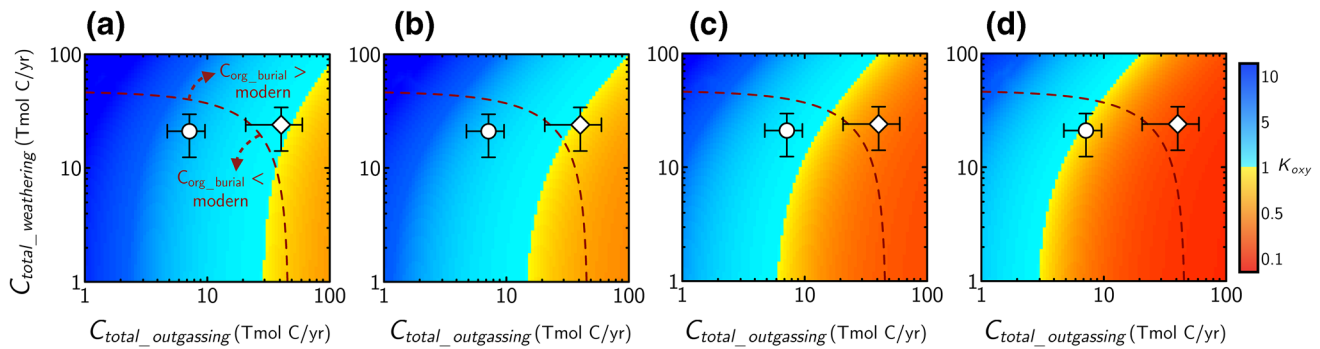


**Figure 9.** Relative Archean oxygenation ( $K_{\text{oxy}}$ ) as a function of weathering and outgassing inputs. Four scenarios depict: (a) nominal Archean case, (b) nominal case modified to account for muted sulfide burial (cf., Holland, 2002), (c) muted sulfide burial plus 1.8 $\times$  increase in outgassing of reductants [= 0.5 log unit decrease in upper mantle  $f(\text{O}_2)$ ], (d) muted sulfide burial plus 3.2 $\times$  increase in outgassing of reductants [= 1.0 log unit decrease in upper mantle  $f(\text{O}_2)$ ]. In all plots, circle denotes modern fluxes, diamond denotes estimated mid-Archean fluxes, and dashed line denotes contour of modern  $C_{\text{org\_burial}}$  flux. Calculations are described in Section 5.2 of the text.

Scenarios C and D). Because  $f(\text{H}_2)$  varies as  $f(\text{O}_2)^{-0.5}$  (Holland, 2002), these changes equate to a difference in redox state of 0.5 and 1.0 log units [i.e., change in oxygen fugacity expressed as  $\Delta f(\text{O}_2)$  relative to the fayalite-magnetite-quartz buffer (FMQ)] between the modern and Archean mantle. This is of similar magnitude to the changes invoked in recent studies (Aulbach & Stagno, 2016; Nicklas et al., 2019), allowing us to assess whether those findings can help resolve the Archean redox budget (though we note that certain factors may complicate the relationship between upper mantle  $f(\text{O}_2)$  and the redox state of outgassed material, for example, changing temperature/pressure conditions in melt-buffered systems, Kadoya et al., 2020c, or garnet fractionation during magmatic differentiation, Tang et al., 2018). Accounting for these potential changes in the redox state of outgassed material gives  $K_{\text{OXY}}$  values of  $0.5^{+0.4}_{-0.1}$  and  $0.3^{+0.2}_{-0.1}$  for our inferred mid-Archean fluxes (Figures 9c and 9d), thereby allowing high rates of organic burial to be reconciled with atmospheric anoxia. We therefore surmise that a stronger flux of reduced gases—due to a shift in the primary locus of volcanism, change in mantle redox state, or other mechanism—could have played a critical role in keeping the Archean atmosphere anoxic despite high burial efficiency.

## 6. Discussion

### 6.1. Assumptions and Caveats

As noted throughout the text, we stress that the calculations presented here are a very simplified view of Earth's surface carbon budget. We have intentionally considered broad ranges for each parameter to capture the large uncertainty associated with each flux estimation. The determination of the most likely values for each parameter, as constrained by empirical data, is not the aim of this study, although such an approach can be taken using Monte Carlo methods (cf. Krissansen-Totton et al., 2018a). Importantly, our simple calculations show that even within these broad uncertainty envelopes—and even when conducting the calculations within different authors' frameworks (Figure 6)—the conclusion remains that traditional estimates of carbon inputs and outputs do not satisfy mass balance in Earth's early history.

We favor high organic burial efficiency in the Precambrian ocean as the resolution to this paradox. This is supported by (i) existing models that argue for high burial efficiency in the Precambrian ocean (Kipp & Stüeken, 2017; Laakso & Schrag, 2018), (ii) the ability of high burial efficiency to account for mass balance even at very high rates of carbon input (Figure 8a), and (iii) the ability of high burial efficiency to be reconciled with a low- $\text{O}_2$  Archean atmosphere (Figure 9). We note, however, that other factors could have also played a role.

For instance, if the “true”  $f_{\text{org}}$  value was lower in the Precambrian than is typically reconstructed from the  $\delta^{13}\text{C}$  record (Section 4.1), this would imply greater total carbon burial than we have inferred in our nominal calculations. As was noted above, recent modeling has suggested that this offset was minor in the Archean

(Krissansen-Totton et al., 2015); however, others have argued for a pronounced offset between “true” and “apparent”  $f_{\text{org}}$  values (Bjerrum & Canfield, 2004; Daines et al., 2017). The discovery of isotopically depleted carbonate in Archean basalts could lend credence to some such hypotheses (Bjerrum & Canfield, 2004). But in the absence of such evidence, we find burial efficiency to be a more likely explanation for high total carbon burial rates than massive changes to fractional organic burial.

## 6.2. Implications for Oxygenation of Early Earth and Earth-Like Exoplanets

The calculations presented may help our understanding of planetary oxygenation, both on the early Earth and Earth-like exoplanets. In particular, we have demonstrated that despite compelling evidence for lower-than-modern NPP in Earth's early history, organic carbon was perhaps buried at higher-than-modern rates due to high burial efficiency (Figure 8). If oxygenic photosynthesis arose  $10^7$ – $10^9$  yr prior to the GOE (cf. Buick, 2008), this would imply a substantial addition of  $\text{O}_2$  equivalents to Earth's surface. As we demonstrated in Section 5.2, such a scenario can in fact be reconciled with atmospheric anoxia in the Archean if reductants were being more effectively outgassed from the mantle at that time.

This finding supports recent modeling work (e.g., Kadoya et al., 2020b), which has demonstrated that the changes in mantle redox state recently inferred from redox-sensitive trace elements in Archean basalts and komatiites (Aulbach & Stagno, 2016; Nicklas et al., 2019) are sufficient to explain the timing and magnitude of the GOE. If organic carbon burial was indeed quite high in the Archean because of elevated burial efficiency (Figure 8), and a change in mantle redox state did indeed trigger the GOE, it would suggest that the timing and tempo of planetary oxygenation is largely dependent on the evolution of the solid Earth. In other words, the permanent oxygenation of Earth's environment may not have been triggered by increased burial of organic carbon derived from oxygenic photosynthesis; instead, a decline in the flux of reductants may have been more important in dictating the timing of the GOE within Earth's evolution.

As habitable exoplanets are studied in increasing numbers, controls on the GOE could inform assessments of the prevalence of oxygenated atmospheres—and correspondingly, complex life (cf. Catling et al., 2005)—on distant Earth-like worlds. In particular, models that can constrain mantle redox evolution on rocky exoplanets using observable parameters (e.g., mass, radius, and stellar metallicity) could become an important component of assessing long-term planetary habitability and the potential for complex life.

## 7. Conclusion

The canonical histories of carbon inputs and outputs from the surface reservoir in Earth's early history create an apparent paradox: most models invoke higher rates of carbon input yet lower carbon burial. We find that higher burial efficiency of organic carbon in Precambrian marine sediments is a probable solution to this imbalance, requiring burial efficiency similar to modern anoxic and low-sulfate settings in order to balance carbon inputs and outputs. By invoking higher organic burial efficiency, high rates of organic carbon burial are implicated (potentially higher than modern rates), which creates a possible conundrum for the Earth's redox budget prior to the GOE. However, we find that it is possible to reconcile high burial efficiency and high organic carbon burial with an anoxic Archean atmosphere, particularly if the flux of oxidizable gases from the mantle was greater in the Archean than it is today. In sum, our calculations suggest that Earth was able to cycle carbon through the surface reservoir more rapidly in the past, despite limited biological productivity. These findings also suggest that mantle redox evolution could have played an important role in determining the timing and tempo of Earth's oxygenation, which may also be true for Earth-like exoplanets.

## Data Availability Statement

No new data were presented in this study. All compiled data are presented in the included figures and tables with accompanying references. All model equations are presented in the main text.

## Acknowledgments

The authors thank Cin-Ty Lee and Katsumi Matsumoto for helpful comments in the review and editorial handling of this manuscript. M. Kipp acknowledges funding from an NSF Graduate Research Fellowship and an Agouron Institute Geobiology Postdoctoral Fellowship. J. Krissansen-Totton was supported by NASA through the NASA Hubble Fellowship grant HF2-51437 awarded by the Space Telescope Science Institute, which is operated by the Association of Universities for Research in Astronomy, Inc. for NASA under contract NASS-26555. David C. Catling acknowledges funding from NSF Frontiers in Earth System Dynamics award 1338810 and NASA Exobiology Program grant NNX15AL23G.

## References

- Anderson, L. A., & Sarmiento, J. L. (1994). Redfield ratios of remineralization determined by nutrient data analysis. *Global Biogeochemical Cycles*, 8(1), 65–80.
- Armstrong, R., & Harmon, R. (1981). Radiogenic isotopes: The case for crustal recycling on a near-steady-state no-continental-growth Earth [and discussion]. *Philosophical Transactions of the Royal Society of London A: Mathematical, Physical and Engineering Sciences*, 301, 443–472.
- Arthur, M. A., Dean, W. E., Neff, E. D., Hay, B. J., King, J., & Jones, G. (1994). Varve calibrated records of carbonate and organic carbon accumulation over the last 2000 years in the Black Sea. *Global Biogeochemical Cycles*, 8(2), 195–217.
- Aulbach, S., & Stagno, V. (2016). Evidence for a reducing Archean ambient mantle and its effects on the carbon cycle. *Geology*, 44(9), 751–754.
- Avice, G., Marty, B., & Burgess, R. (2017). The origin and degassing history of the Earth's atmosphere revealed by Archean xenon. *Nature Communications*, 8, 15455.
- Bekker, A., & Holland, H. D. (2012). Oxygen overshoot and recovery during the early Paleoproterozoic. *Earth and Planetary Science Letters*, 317, 295–304.
- Berner, R. A. (1973). Phosphate removal from sea water by adsorption on volcanogenic ferric oxides. *Earth and Planetary Science Letters*, 18(1), 77–86.
- Berner, R. A. (1991). A model for atmospheric CO<sub>2</sub> over Phanerozoic time. *American Journal of Science*, 291, 339–376.
- Berner, R. A. (2004). *The Phanerozoic carbon cycle: CO<sub>2</sub> and O<sub>2</sub>*. Oxford University Press.
- Berner, R. A., & Caldeira, K. (1997). The need for mass balance and feedback in the geochemical carbon cycle. *Geology*, 25(10), 955–956.
- Bjerrum, C. J., & Canfield, D. E. (2002). Ocean productivity before about 1.9 Gyr ago limited by phosphorus adsorption onto iron oxides. *Nature*, 417(6885), 159–162.
- Bjerrum, C. J., & Canfield, D. E. (2004). New insights into the burial history of organic carbon on the early Earth. *Geochemistry, Geophysics, Geosystems*, 5, Q08001. <https://doi.org/10.1029/2004GC000713>
- Blake, R. E., Chang, S. J., & Lepland, A. (2010). Phosphate oxygen isotopic evidence for a temperate and biologically active Archean ocean. *Nature*, 464, 1029–1032.
- Bluth, G. J. S., & Kump, L. R. (1991). Phanerozoic paleogeology. *American Journal of Science*, 291, 284–308.
- Bolton, E. W., Berner, R. A., & Petsch, S. T. (2006). The weathering of sedimentary organic matter as a control on atmospheric O<sub>2</sub>: II. Theoretical modeling. *American Journal of Science*, 306(8), 575–615.
- Buick, R. (2008). When did oxygenic photosynthesis evolve? *Philosophical Transactions of the Royal Society B: Biological Sciences*, 363(1504), 2731–2743.
- Campbell, I. H. (2003). Constraints on continental growth models from Nb/U ratios in the 3.5 Ga Barberton and other Archean basalt-komatiite suites. *American Journal of Science*, 303, 319–351.
- Canfield, D. E. (1998). A new model for Proterozoic ocean chemistry. *Nature*, 396(6710), 450–453.
- Canfield, D. E., Rosing, M. T., & Bjerrum, C. (2006). Early anaerobic metabolisms. *Philosophical Transactions: Biological Science*, 361(1474), 1819–1836.
- Canil, D. (1997). Vanadium partitioning and the oxidation state of Archean komatiite magmas. *Nature*, 389(6653), 842.
- Cartigny, P. (2005). Stable isotopes and the origin of diamond. *Elements*, 1, 79–84.
- Catling, D. C., Glein, C. R., Zahnle, K. J., & McKay, C. P. (2005). Why O<sub>2</sub> is required by complex life on habitable planets and the concept of planetary “oxygenation time”. *Astrobiology*, 5, 415–438.
- Catling, D. C., & Kasting, J. F. (2017). *Atmospheric evolution on inhabited and lifeless worlds*. Cambridge University Press.
- Catling, D. C., & Zahnle, K. J. (2020). The Archean atmosphere. *Science Advances*, 6, eaax1420.
- Chang, S., & Berner, R. A. (1999). Coal weathering and the geochemical carbon cycle. *Geochimica et Cosmochimica Acta*, 63, 3301–3310.
- Claire, M. W., Catling, D. C., & Zahnle, K. J. (2006). Biogeochemical modelling of the rise in atmospheric oxygen. *Geobiology*, 4(4), 239–269.
- Crockford, P. W., Hayles, J. A., Bao, H., Planavsky, N. J., Bekker, A., Fralick, P. W., et al. (2018). Triple oxygen isotope evidence for limited mid-Proterozoic primary productivity. *Nature*, 559, 613–616.
- Daines, S. J., Mills, B. J., & Lenton, T. M. (2017). Atmospheric oxygen regulation at low Proterozoic levels by incomplete oxidative weathering of sedimentary organic carbon. *Nature Communications*, 8, 14379.
- Dasgupta, R., & Hirschmann, M. M. (2010). The deep carbon cycle and melting in Earth's interior. *Earth and Planetary Science Letters*, 298(1–2), 1–13.
- Davies, G. F. (2009). Effect of plate bending on the Urey ratio and the thermal evolution of the mantle. *Earth and Planetary Science Letters*, 287(3–4), 513–518.
- Deines, P. (2002). The carbon isotope geochemistry of mantle xenoliths. *Earth-Science Reviews*, 58, 247–278. <https://doi.org/10.1002/2014GC005656>
- Derry, L. A. (2014). Organic carbon cycling and the lithosphere. *Treatise on Geochemistry*, 2, 239–249.
- Derry, L. A. (2015). Causes and consequences of mid-Proterozoic anoxia. *Geophysical Research Letters*, 42(20), 8538–8546. <https://doi.org/10.1002/2015GL065333>
- Des Marais, D. J., Strauss, H., Summons, R. E., & Hayes, J. M. (1992). Carbon isotope evidence for the stepwise oxidation of the Proterozoic environment. *Nature*, 359(6396), 605–609.
- Driese, S. G., Jirsa, M. A., Ren, M., Brantley, S. L., Sheldon, N. D., Parker, D., & Schmitz, M. (2011). Neoproterozoic paleoweathering of tonalite and metabasalt: Implications for reconstructions of 2.69 Ga early terrestrial ecosystems and paleoatmospheric chemistry. *Precambrian Research*, 189, 1–17.
- Duncan, M. S., & Dasgupta, R. (2017). Rise of Earth's atmospheric oxygen controlled by efficient subduction of organic carbon. *Nature Geoscience*, 10, 387–392.
- Farquhar, J., Bao, H. M., & Thieme, M. (2000). Atmospheric influence of Earth's earliest sulfur cycle. *Science*, 289(5480), 756–758.
- Feely, R. A., Trefry, J. H., Lebon, G. T., & German, C. R. (1998). The relationship between P/Fe and V/Fe ratios in hydrothermal precipitates and dissolved phosphate in seawater. *Geophysical Research Letters*, 25(13), 2253–2256.
- Feulner, G. (2012). The faint young Sun problem. *Reviews of Geophysics*, 50, RG2006. <https://doi.org/10.1029/2011RG000375>
- Field, C. B., Behrenfeld, M. J., Randerson, J. T., & Falkowski, P. (1998). Primary production of the biosphere: Integrating terrestrial and oceanic components. *Science*, 281(5374), 237–240.
- Flament, N., Coltice, N., & Rey, P. F. (2008). A case for late-Archean continental emergence from thermal evolution models and hypsometry. *Earth and Planetary Science Letters*, 275, 326–336.

- Gaillardet, J., Calmels, D., Romero-Mujalli, G., Zakharova, E., & Hartmann, J. (2019). Global climate control on carbonate weathering intensity. *Chemical Geology*, 527, 118762.
- Gaillardet, F., Scailliet, B., & Arndt, N. T. (2011). Atmospheric oxygenation caused by a change in volcanic degassing pressure. *Nature*, 478, 229–232.
- Godderis, Y., & Veizer, J. (2000). Tectonic control of chemical and isotopic composition of ancient oceans; the impact of continental growth. *American Journal of Science*, 300(5), 434–461.
- Gough, D. (1981). Solar interior structure and luminosity variations. *Solar Physics*, 74(1), 21–34.
- Gumsley, A. P., Chamberlain, K. R., Bleeker, W., Söderlund, U., Kock, M. O. de, Larsson, E. R., & Bekker, A. (2017). Timing and tempo of the Great Oxidation Event. *Proceedings of the National Academy of Sciences of the United States of America*, 114(8), 1811–1816.
- Halevy, I., Alesker, M., Schuster, E. M., Popovitz-Biro, R., & Feldman, Y. (2017). A key role for green rust in the Precambrian oceans and the genesis of iron formations. *Nature Geoscience*, 10(2), 135–139.
- Hawkesworth, C. J., Cawood, P. A., Dhuime, B., & Kemp, T. I. S. (2017). Earth's continental lithosphere through time. *Annual Review of Earth and Planetary Sciences*, 45, 169–198.
- Hedges, J. I., & Keil, R. G. (1995). Sedimentary organic matter preservation: An assessment and speculative synthesis. *Marine Chemistry*, 49(2–3), 81–115.
- Hodgskiss, M. S. W., Crockford, P. W., Peng, Y., Wing, B. A., & Horner, T. J. (2019). A productivity collapse to end Earth's Great Oxidation. *Proceedings of the National Academy of Sciences of the United States of America*, 116(35), 17207–17212.
- Holland, H. D. (1978). *The chemistry of the atmosphere and oceans*. Wiley.
- Holland, H. D. (1984). *The chemical evolution of the atmosphere and oceans*. Princeton University Press.
- Holland, H. D. (2002). Volcanic gases, black smokers, and the Great Oxidation Event. *Geochimica et Cosmochimica Acta*, 66(21), 3811–3826.
- Holland, H. D. (2009). Why the atmosphere became oxygenated: A proposal. *Geochimica et Cosmochimica Acta*, 73(18), 5241–5255.
- Holser, W. T., Schidlowski, M., Garrels, R. M., MacKenzie, F. T., & Maynard, J. B. (1988). Geochemical cycles of carbon and sulfur. In *Chemical cycles in the evolution of the Earth* C. B. Gregor (pp. 105–173). New York, NY: John Wiley.
- Hren, M., Tice, M., & Chamberlain, C. (2009). Oxygen and hydrogen isotope evidence for a temperate climate 3.42 billion years ago. *Nature*, 462, 205–208.
- Jones, C., Nomosatryo, S., Crowe, S. A., Bjerrum, C. J., & Canfield, D. E. (2015). Iron oxides, divalent cations, silica, and the early earth phosphorus crisis. *Geology*, 43(2), 135–138.
- Kadoya, S., Krissansen-Totton, J., & Catling, D. C. (2020a). Probable cold and alkaline surface environment of the Hadean Earth caused by impact ejecta weathering. *Geochemistry, Geophysics, Geosystems*, 21, e2019GC008734. <https://doi.org/10.1029/2019GC008734>
- Kadoya, S., Catling, D. C., Nicklas, R. W., Puchtel, I. S., & Anbar, A. D. (2020b). Mantle data imply a decline of oxidizable volcanic gases could have triggered the Great Oxidation Event. *Nature Communications*, 11, 2774.
- Kadoya, S., Catling, D. C., Nicklas, R. W., Puchtel, I. S., & Anbar, A. D. (2020c). Mantle cooling causes more reducing volcanic gases and gradual reduction of the atmosphere. *Geochemical Perspectives Letters*, 13, 25–29.
- Kah, L. C., & Riding, T. (2007). Mesoproterozoic carbon dioxide levels inferred from calcified cyanobacteria. *Geology*, 35, 799–802.
- Kanzaki, Y., & Murakami, T. (2015). Estimates of atmospheric CO<sub>2</sub> in the Neoproterozoic from paleosols. *Geochimica et Cosmochimica Acta*, 159, 190–219.
- Kasting, J. F. (2013). What caused the rise of atmospheric O<sub>2</sub>? *Chemical Geology*, 362, 13–25.
- Kasting, J. F., Catling, D. C., & Zahnle, K. (2012). Atmospheric oxygenation and volcanism. *Nature*, 487, E12012.
- Kharecha, P., Kasting, J., & Siefert, J. (2005). A coupled atmosphere-ecosystem model of the early Archean Earth. *Geobiology*, 3(2), 53–76.
- Kipp, M. A., & Stüeken, E. E. (2017). Biomass recycling and Earth's early phosphorus cycle. *Science Advances*, 3(11), eaao4795.
- Konhauser, K. O., Lalonde, S. V., Amskold, L., & Holland, H. D. (2007). Was there really an Archean phosphate crisis? *Science*, 315(5816), 1234.
- Korenaga, J. (2006). Archean geodynamics and the thermal evolution of Earth. *Geophysical Monograph-American Geophysical Union*, 164, 7. <https://doi.org/10.1029/164GM03>
- Korenaga, J. (2009). Scaling of stagnant-lid convection with Arrhenius rheology and the effects of mantle melting. *Geophysical Journal International*, 179, 154–170. <https://doi.org/10.1111/j.1365-246X.2009.04272.x>
- Krissansen-Totton, J., Arney, G. N., & Catling, D. C. (2018a). Constraining the climate and ocean pH of the early Earth with a geological carbon cycle model. *Proceedings of the National Academy of Sciences of the United States of America*, 115(16), 4105–4110.
- Krissansen-Totton, J., Buick, R., & Catling, D. C. (2015). A statistical analysis of the carbon isotope record from the Archean to Phanerozoic and implications for the rise of oxygen. *American Journal of Science*, 315(4), 275–316.
- Krissansen-Totton, J., & Catling, D. C. (2017). Constraining climate sensitivity and continental versus seafloor weathering using an inverse geological carbon cycle model. *Nature Communications*, 8, 1–15.
- Krissansen-Totton, J., Olson, S., & Catling, D. C. (2018b). Disequilibrium biosignatures over Earth history and implications for detecting exoplanet life. *Science Advances*, 4, eaao5747.
- Kump, L. R., & Barley, M. E. (2007). Increased subaerial volcanism and the rise of atmospheric oxygen 2.5 billion years ago. *Nature*, 448(7157), 1033–1036.
- Kuntz, L. B., Laakso, T. A., Schrag, D. P., & Crowe, S. A. (2015). Modeling the carbon cycle in Lake Matano. *Geobiology*, 13(5), 454–461.
- Laakso, T. A., & Schrag, D. P. (2018). Limitations on limitation. *Global Biogeochemical Cycles*, 32(3), 486–496.
- Lasaga, A. C., & Ohmoto, H. (2002). The oxygen geochemical cycle: Dynamics and stability. *Geochimica et Cosmochimica Acta*, 66, 361–381.
- Lee, C.-T. A., Yeung, L. Y., McKenzie, N. R., Yokoyama, Y., Ozaki, K., & Lenardic, A. (2016). Two-step rise of atmospheric oxygen linked to the growth of continents. *Nature Geoscience*, 9(6), 417–424.
- Lenton, T. M., Daines, S. J., & Mills, B. J. W. (2018). COPSE reloaded: An improved model of biogeochemical cycling over Phanerozoic time. *Earth-Science Reviews*, 178, 1–28.
- Li, Z.-X. A., & Lee, C.-T. A. (2004). The constancy of upper mantle fO<sub>2</sub> through time inferred from V/Sc ratios in basalts. *Earth and Planetary Science Letters*, 228(3–4), 483–493.
- Luz, B., Barkan, E., Bender, M. L., Thieme, M. H., & Boering, K. A. (1999). Triple-isotope composition of atmospheric oxygen as a tracer of biosphere productivity. *Nature*, 400, 547–550.
- Lyons, T. W., Reinhard, C. T., & Planavsky, N. J. (2014). The rise of oxygen in Earth's early ocean and atmosphere. *Nature*, 506, 307–315.
- Marty, B., Bekaert, D. V., Broadley, M. W., & Jaupart, C. (2019). Geochemical evidence for high volatile fluxes from the mantle at the end of the Archaean. *Nature*, 575, 485–488.
- Mattey, D. P. (1987). Carbon isotopes in the mantle. *Terra Cognita*, 7, 31–37.
- McLennan, S. M., & Taylor, S. (1982). Geochemical constraints on the growth of the continental crust. *Journal of Geology*, 90, 347–361.

- Middelburg, J. J. (2019). Carbon processing at the seafloor. *Marine carbon biogeochemistry* (pp. 57–75). Cham: Springer.
- Nakamura, K., & Kato, Y. (2004). Carbonatization of oceanic crust by the seafloor hydrothermal activity and its significance as a CO<sub>2</sub> sink in the Early Archean. *Geochimica et Cosmochimica Acta*, 68(22), 4595–4618.
- Nicklas, R. W., Puchtel, I. S., Ash, R. D., Piccoli, P. M., Hanski, E. J., Nisbet, E. G., et al. (2019). Secular mantle oxidation across the Archean-Proterozoic boundary: Evidence from V partitioning in komatiites and picrites. *Geochimica et Cosmochimica Acta*, 250, 49–75.
- Pavlov, A. A., & Kasting, J. F. (2002). Mass-independent fractionation of sulfur isotopes in Archean sediments: Strong evidence for an anoxic Archean atmosphere. *Astrobiology*, 2(1), 27–41.
- Pearson, D. G., Canil, D., & Shirey, S. B. (2014). Mantle samples included in volcanic rocks: Xenoliths and diamonds. *Treatise on Geochemistry*, 2, 568.
- Poulton, S. W., Fralick, P. W., & Canfield, D. E. (2004). The transition to a sulphidic ocean ~1.84 billion years ago. *Nature*, 431(7005), 173.
- Ramos, R. J., Lackey, J. S., Barnes, J. D., & Fulton, A. A. (2020). Remnants and rates of metamorphic decarbonation in continental arcs. *Geological Society of America Today*, 30, 4–10.
- Rasmussen, B., Krapež, B., Muhling, J. R., & Suvorova, A. (2015). Precipitation of iron silicate nanoparticles in early Precambrian oceans marks Earth's first iron age. *Geology*, 43(4), 303–306.
- Rasmussen, B., Meier, D. B., Krapež, B., & Muhling, J. R. (2013). Iron silicate microgranules as precursor sediments to 2.5-billion-year-old banded iron formations. *Geology*, 41(4), 435–438.
- Redfield, A. C. (1958). The biological control of chemical factors in the environment. *American Scientist*, 46, 205–221.
- Reinhard, C. T., Olson, S. L., Schwieterman, E. W., & Lyons, T. W. (2017a). False negatives for remote life detection on ocean-bearing planets: Lessons from the early Earth. *Astrobiology*, 17(4), 287–297.
- Reinhard, C. T., Planavsky, N. J., Gill, B. C., Ozaki, K., Robbins, L. J., Lyons, T. W., et al. (2017b). Evolution of the global phosphorus cycle. *Nature*, 541, 386–389.
- Reymer, A., & Schubert, G. (1984). Phanerozoic addition rates to the continental crust and crustal growth. *Tectonics*, 3, 63–77.
- Romero-Mujalli, G., Hartmann, J., Borker, J., Gaillardet, J., & Calmels, D. (2019). Ecosystem controlled soil-rock pCO<sub>2</sub> and carbonate weathering – Constraints by temperature and soil water content. *Chemical Geology*, 527, 118634.
- Sagan, C., & Mullen, G. (1972). Earth and mars – Evolution of atmospheres and surface temperatures. *Science*, 177(4043), 52–56.
- Schidlowski, M. (2001). Carbon isotopes as biogeochemical recorders of life over 3.8 Ga of earth history: Evolution of a concept. *Precambrian Research*, 106(1), 117–134.
- Schlesinger, W. H., & Bernhardt, E. S. (2013). *Biogeochemistry: An analysis of global change* (3rd ed.). Academic Press.
- Schrag, D. P., Higgins, J. A., Macdonald, F. A., & Johnston, D. T. (2013). Authigenic carbonate and the history of the global carbon cycle. *Science*, 339(6119), 540–543.
- Scott, C. T., Bekker, A., Reinhard, C. T., Schmetzger, B., Krapež, B., Rumble, D., & Lyons, T. W. (2011). Late Archean euxinic conditions before the rise of atmospheric oxygen. *Geology*, 39(2), 119–122.
- Sheldon, N. D. (2006). Precambrian paleosols and atmospheric CO<sub>2</sub> levels. *Precambrian Research*, 147, 148–155.
- Shirey, S. B., Cartigny, P., Frost, D. J., Keshav, S., Nestola, F., Nimis, P., et al. (2013). Diamonds and the geology of mantle carbon. *Reviews in Mineralogy and Geochemistry*, 75, 355–421.
- Sigman, D. M., & Hain, M. P. (2012). The biological productivity of the ocean. *Nature Education*, 3(6), 1–16.
- Sleep, N. H., & Zahnle, K. (2001). Carbon dioxide cycling and implications for climate on ancient Earth. *Journal of Geophysical Research*, 106(E1), 1373–1399.
- Stüeken, E. E., Kipp, M. A., Koehler, M. C., Schwieterman, E. W., Johnson, B. W., & Buick, R. (2016). Modeling pN<sub>2</sub> through geological time: Implications for planetary climates and atmospheric biosignatures. *Astrobiology*, 16(12), 949–963.
- Tang, M., Erdman, M., Eldridge, G., & Lee, C.-T. A. (2018). The redox “filter” beneath magmatic orogens and the formation of continental crust. *Science Advances*, 4, eaar4444.
- Tanioka, T., & Matsumoto, K. (2020). Stability of marine organic matter respiration stoichiometry. *Geophysical Research Letters*, 47, e2019GL085564. <https://doi.org/10.1029/2019GL085564>
- Trail, D., Watson, E. B., & Tailby, N. D. (2011). The oxidation state of Hadean magmas and implications for early Earth's atmosphere. *Nature*, 480(7375), 79.
- Tyrrell, T. (1999). The relative influences of nitrogen and phosphorus on oceanic primary production. *Nature*, 400(6744), 525–531.
- Veizer, J., & Jansen, S. L. (1979). Basement and sedimentary recycling and continental evolution. *Journal of Geology*, 87, 341–370.
- Walker, J. C. G., Hays, P. B., & Kasting, J. F. (1981). A negative feedback mechanism for the long-term stabilization of Earth's surface temperature. *Journal of Geophysical Research*, 86(C10), 9776–9782.
- Ward, L. M., Rasmussen, B., & Fischer, W. W. (2019). Primary productivity was limited by electron donors prior to the advent of oxygenic photosynthesis. *Journal of Geophysical Research: Biogeosciences*, 124(2), 211–226. <https://doi.org/10.1029/2018JG004679>
- Warke, M. R., DiRocco, T., Zerkle, A. L., Lepland, A., Prave, A. R., Martin, A. P., et al. (2020). The Great Oxidation Event preceded a Paleoproterozoic “snowball Earth”. *Proceedings of the National Academy of Sciences of the United States of America*, 117, 13314–13320.
- White, A. E., Spitz, Y. H., Karl, D. M., & Letelier, R. M. (2006). Flexible elemental stoichiometry in *Trichodesmium* spp. an its ecological implications. *Limnology and Oceanography*, 51(4), 1777–1790.
- Zahnle, K. J., Claire, M. W., & Catling, D. C. (2006). The loss of mass-independent fractionation in sulfur due to a Palaeoproterozoic collapse of atmospheric methane. *Geobiology*, 4, 271–283.